IDEA

Innovations Deserving Exploratory Analysis Programs

NCHRP IDEA Program

MILDGLASS: GFRP Strand for Resilient Mild Pre-Stressed Concrete

Final Report for
NCHRP IDEA Project 207

Prepared by:
Marco Rossini
Antonio Nanni
University of Miami

May 2020

TRANSPORTATION RESEARCH BOARD
The National Academies of
SCIENCES · ENGINEERING · MEDICINE

Innovations Deserving Exploratory Analysis (IDEA) Programs Managed by the Transportation Research Board

This IDEA project was funded by the NCHRP IDEA Program.

The TRB currently manages the following three IDEA programs:

- The NCHRP IDEA Program, which focuses on advances in the design, construction, and maintenance of highway systems, is funded by American Association of State Highway and Transportation Officials (AASHTO) as part of the National Cooperative Highway Research Program (NCHRP).
- The Safety IDEA Program currently focuses on innovative approaches for improving railroad safety or performance. The program is currently funded by the Federal Railroad Administration (FRA). The program was previously jointly funded by the Federal Motor Carrier Safety Administration (FMCSA) and the FRA.
- The Transit IDEA Program, which supports development and testing of innovative concepts and methods for advancing transit practice, is funded by the Federal Transit Administration (FTA) as part of the Transit Cooperative Research Program (TCRP).

Management of the three IDEA programs is coordinated to promote the development and testing of innovative concepts, methods, and technologies.

For information on the IDEA programs, check the IDEA website (www.trb.org/idea). For questions, contact the IDEA programs office by telephone at (202) 334-3310.

IDEA Programs
Transportation Research Board
500 Fifth Street, NW
Washington, DC 20001

MILDGLASS: GFRP Strand for Resilient Mild Pre-Stressed Concrete

IDEA Program Final Report

NCHRP-IDEA/207

Prepared for the IDEA Program
Transportation Research Board
The National Academies

Marco Rossini
Antonio Nanni

University of Miami

Submitted on February 24, 2020
Submitted with revision on May 25, 2020

ACKNOWLEDGEMENTS

The authors gratefully acknowledge the financial support from: (1) "MILDGLASS: GFRP Strand for Resilient Mild Prestressed Concrete" Transportation Research Board of the National Academies of Sciences, Engineering, and Medicine, NCHRP-IDEA/207; (2) "HuRRI-Composites: Resilient Coastal Communities Using Advanced Construction Materials and Systems" Hurricane Resilience Research Institute; (3) "CICI: Center for the Integration of Composites into Infrastructure" National Science Foundation, I/UCRC:1439543; and, (4) Zegna Foundation for supporting Dr. Marco Rossini's research activity in the field of composite materials for infrastructural applications.

The research team at the University of Miami (UM) included: Dr. Antonio Nanni, Dr. Marco Rossini, Gianluca Pulvirenti, Niccolò Braghiroli, Pedro Jalles, Nafiseh Kiani, Christian Steputat, Roberto Rodriguez, Alvaro Ruiz Emparanza, Dr. Thomas Cadenazzi, Dr. Guillermo Claure, and Dr. Francisco De Caso y Basalo. Dr. Marco Rossini's affiliation to the University of Miami ended in December 2019 as of his graduation. Prof. Giovanni Dotelli at Politecnico di Milano provided consulting concerning Life Cycle Cost (LCC) Analysis. Dr. Saverio Spadea at the University of Dundee provided consulting concerning the modelling and mechanical performance of composite material. Prof. Carlo Poggi at Politecnico di Milano provided consulting concerning the mechanical behavior of composite material and their statistical modelling. Part of the experimental activities reported in Part 3 of this report were conducted at the University of Texas at Tyler under the supervision of Dr. Michael Gangone and funded by "HuRRI-Composites: Resilient Coastal Communities Using Advanced Construction Materials and Systems" a seed grant awarded by the Hurricane Resilience Research Institute. The structural tests reported in Part 5 of this report were conducted at the University of Houston (UH) under the supervision of Dr. Abdeldjelil Belarbi and funded by "HuRRI-Composites: Resilient Coastal Communities Using Advanced Construction Materials and Systems" a seed grant awarded by the Hurricane Resilience Research Institute. The creep-rupture database analyzed in Part 4 of this study was partly assembled at the University of Sherbrooke under the supervision of Dr. Brahim Benmokrane [1], and partly assembled at the American University in Dubai under the supervision of Dr. Elias Saqan [2].

Several industrial partners were involved in this project. SIREG contributed as a composite material manufacturer committing technical resources, funding, and personnel to the development of the Glass Fiber Reinforced Polymer (GFRP) tendons and part of the anchoring systems discussed in Part 1, Part 2, and Part 3 of this report. Furthermore, SIREG donated material for testing, including the structural tests discussed in Part 5 of this report, and for the construction of the demonstrator discussed in Part 6 of this report. Arkema contributed as a resin manufacturer, committing technical resources, funding, and personnel to the development of part of the GFRP tendons discussed in Part 2 and Part 3 of this report. Owens Corning contributed as a glass fiber and GFRP bars manufacturer providing technical support and donating part of the reinforcement for the construction of the demonstrator discussed in Part 6 of this report. Gate Precast Company contributed as a precaster committing facilities, resources, material, and personnel to the construction of the demonstrative piles discussed in Part 6 of this report. Anzac Contractors contributed as a general contractor providing technical support and allowing and supporting monitoring of the installation phases of the demonstrator discussed in Part 6 of this report. Buzzi Unicem contributed as a cement manufacturer and ready mix producer providing technical support and consultancy.

The authors gratefully acknowledge the valuable feedback, technical support, and advising of the members of the advisory panel: Steven Nolan at the Florida Department of Transportation (FDOT) (panel chair), William Potter at FDOT and AASHTO Committee T6, Timothy Bradberry at the Texas Department of Transportation (TxDOT), Jamal Elkaissi at the Federal Highway Administration (FHWA), Dr. Fabio Matta at the University of South Carolina (USC), and Thomas Newton at Gate Precast.

TABLE OF CONTENTS

EXECUTIVE SUMMARY

Corrosion of steel reinforcement is the primary cause of durability problems in Reinforced- and Prestressed-Concrete (RC and PC) structures. The legacy of the extensive transportation infrastructure development and expansion, in combination with aggressive environments, represents a critical Maintenance, Rehabilitation and Replacement (MRR) liability at the national scale. RC corrosion is ubiquitous, but greatly exacerbated by the aggressive sub-tropical environments of southern coastal states as well as exposure to the aggression of de-icing agents and carbonation in cold-weather northern regions. In the case of transportation infrastructure in coastal areas, the immediate corrosion problems are experienced by bridge substructures, sheet pile bulkheads and seawalls. For the latter structures typically made with PC elements, the preference for non-corrosive reinforcement is explicitly stated by the Florida Department of Transportation (FDOT) among the others. In the State of Florida alone, about 3,600 coastal miles are armored with aging sheet piles with an estimated $21B MRR liability.

The construction industry has only partially answered the rising demand for corrosion-resistant technologies, offering expensive, complex and sometimes ineffective solutions. This project developed corrosion-resistant tendons for PC application that, in addition to durability and mechanical performance, exhibits favorable constructability and cost characteristics. The focus of this project is on Glass Fiber Reinforced Polymer (GFRP) that retains immunity to corrosion and maintains a material cost comparable to traditional carbon steel reinforcement ($1.15/ft.) while also showing higher strain at failure (2.0% ultimate elongation) and lower modulus of elasticity (about 45 GPa) with respect to other non-corrosive reinforcing solutions such as High Strength Stainless Steel (HSSS) and Carbon FRP (CFRP). The low modulus is an advantageous feature in PC construction during fabrication (larger and more controllable displacement at prestressing) and design (lower elastic shortening). It may be argued that the lower creep-rupture strength exhibited by GFRP compared to CFRP and HSSS does not allow designing for the same level of prestressing. However, mild-prestressing presents the advantage to lower losses due to concrete creep during the service life of PC structures. Furthermore, limiting the initial level of prestress addresses the main constructability issues observed with CFRP. It guarantees compatibility with simple prestressing chucks and conventional tensioning techniques. At the same time, the reduced cost of glass fiber makes GFRP reinforcement a competitive and durable alternative to standard low-relaxation High-Strength Carbon Steel (HSCS).

Traditional GFRP solid rebars used in RC construction are typically not suited for prestressing due to their difficulty to be coiled, while a GFRP tendon is currently not available in the marketplace. This project considered and developed various GFRP material solutions that are coilable and may be used in prestressing applications. These include: (a) a 15.2-mm 7-wire GFRP strand prototype developed using Electrical/Chemical Resistant (ECR) glass fibers and thermosetting Vinyl Ester resin (VE) shown at the top left of Figure 1; (b) a 15.2-mm -wire GFRP strand prototype developed using ECR glass fibers and ThermoPlastic (TP) acrylic resin shown at the top right of Figure 1; (c) a 12.7-mm (M13) coilable GFRP bar made with ECR glass fibers and VE resin shown at the bottom left of Figure 1; and, (d) a 12-mm bendable GFRP bar made with ECR glass fibers and TP resin shown at the bottom right of Figure 1. Non-coilable 15.9-mm (M16) GFRP bars made with ECR glass fibers and VE resin were also tested and may be used in smaller scale projects. Two different anchoring systems were evaluated: traditional Steel (ST) prestressing anchors, and an equivalent anchoring system that uses polymeric Nylon (NY) wedges that have a softer interaction with the surface of the reinforcement. The application of a thin layer of Epoxy (EP) coating was also investigated for additional protection during pulling.

The use of TP resin is an innovative solution that eases manufacturing of complex shapes such as 7-wire strands or bent bars by allowing thermoforming, post-heating, and staged manufacturing. It may have a disruptive impact on the composite reinforcement industry providing effective and efficient solutions to foster the durability of transportation infrastructures. The innovation associated with the use of TP resin in GFRP reinforcement was recognized by the 2019 JEC Innovation Award in Construction and Infrastructures presented to a joint partnership of Arkema, the National Cooperative Highway Research Program (NCHRP), SIREG, and the University of Miami for the work developed within the MILDGLASS project. JEC Group is the world's leading company dedicated to the development and promotion of the composite industry. Beyond the immediate purpose of this project, the use of thermoplastic resin can also have relevant implications on the GFRP reinforcement supply chain. Given that within the steel industry, a steel mill is not responsible for shaping and cutting bars to order. Instead, a bar fabricator stocks large quantity of coiled straight bars that are readily shaped and cut once orders are received from the construction site. The use of thermoplastic resin would allow the production of stocks of coiled FRP bars that can be subsequently heated, shaped, and cut to length as orders are received. This solution would sensibly speed up the delivery of complex shapes to the construction field and may allow the manufacturing of higher-quality reinforcement with positive implications on the overall performance of GFRP-MPC structural members.

The project had a duration of 2 years and was subdivided into two stages. Stage I focused on the development, testing, and characterization of GFRP coilable material systems for concrete prestressing. Stage II focuses on the design, construction, and testing of demonstrative structures using pre-tensioned GFRP reinforcement. Of the four coilable material systems considered, M13 VE-GFRP coilable bars coupled with NY wedges proved ready for field deployment in pre-tensioning projects at a pull of 30 kN after seating losses, corresponding to approximately 30% of the Guaranteed Tensile Strength (GTS) of the bar per ASTM D7957. The other material systems investigated showed promising performance in laboratory conditions and have been developed at a prototypical stage. Experimental testing of the four coilable GFRP material systems showed initial pull strengths ranging from 62 kN to 94 kN (452 MPa to 675 MPa) depending on the material system and the type of anchor considered. Displacement-controlled tests under sustained pull were performed to simulate the behavior of the reinforcement-anchor systems during pre-tensioning operations at a typical precast yard. Tests were conducted at different time durations ranging from 12 hours at 45 kN (348 MPa) on VE-GFRP strands to 7 days at 38 kN (294 MPa) on VE-GFRP M13 straight bars. Results showed compatibility with traditional pulling procedures.

Several industrial partners were involved in this project and maintain their commitment to leverage the diffusion of the technology. This includes SIREG as an FRP manufacturer, Arkema as a resin manufacturer, Owens Corning as a glass fiber and GFRP bars manufacturer, Gate Precast Company as a precaster, and Buzzi Unicem as a cement manufacturer and ready mix producer. FDOT, a key stake holder, is the first utilizer of the technology leading a nation-wide pre-standardization effort. Two demonstrative piles partially-prestressed using coilable M13 VE-GFRP straight bars have been constructed for installation at the FDOT-managed 23rd Avenue Bridge over Ibis Waterway in Broward County, FL (Figure 2). The last component of this study quantified the economic implications of the technology. Projections show how a GFRP partially prestressed pile may feature an initial cost at approximately two thirds of a CFRP- or HSSS-prestressed pile and a Life Cycle Cost (LCC) approximately 30% lower than a traditional pile prestressed using carbon steel strands.

Figure 1 – GFRP/VE 15.2-mm strand compared to a CFRP commercial solution (top left), 15.2-mm GFRP/TP strand (top right), GFRP/VE 12-mm coilable bar (bottom left), GFRP/TP 12-mm coilable bar (bottom right).

Figure 2 – Construction of two partially-prestressed piles serving as demonstrator for the MILDGLASS concept.

IDEA PRODUCT

This project develops corrosion-resistant tendons for PC application that, in addition to durability and mechanical performance, exhibits favorable constructability and cost characteristics. These Glass Fiber Reinforced Polymer (GFRP) tendons address the need of State Transportation Agencies for cost-effective corrosion-resistant prestressing systems. These tendons are coilable, shippable and compatible with traditional techniques applied to steel-PC tensioning and construction. The focus of this project is on Glass Fiber Reinforced Polymer (GFRP) that retains immunity to corrosion and maintains a material cost comparable to traditional carbon steel reinforcement ($1.15/ft.) while also showing higher strain at failure (2.0% ultimate elongation) and lower modulus of elasticity (approximately 45 GPa) with respect to other non-corrosive reinforcing solutions such as High Strength Stainless Steel (HSSS) and Carbon FRP (CFRP). The low modulus is an advantageous feature in PC construction during fabrication (larger and more controllable displacement at prestressing) and design (lower elastic shortening).

Traditional GFRP solid rebars used in RC construction are typically not suited for prestressing due to their inability to be coiled, while a GFRP tendon is currently not available in the marketplace. This project considers and develops various GFRP material solutions that are coilable and may be used in prestressing applications. These include: (a) a 15.2-mm 7-wire GFRP strand prototype developed using Electrical/Chemical Resistant (ECR) glass fibers and thermosetting Vinyl Ester resin (VE) shown at the top left of Figure 1; (b) a 15.2-mm 7-wire GFRP strand prototype developed using ECR glass fibers and ThermoPlastic (TP) acrylic resin shown at the top right of Figure 1; (c) a 12.7-mm (M13) coilable GFRP bar made with ECR glass fibers and VE resin shown at the bottom left of Figure 1; and, (d) a 12-mm bendable GFRP bar made with ECR glass fibers and TP resin shown at the bottom right of Figure 1. Non-coilable 15.9-mm (M16) GFRP bars made with ECR glass fibers and VE resin were also tested and may be used in smaller scale projects. Two different anchoring systems were considered: traditional Steel (ST) prestressing anchors, and an equivalent anchoring system that uses polymeric Nylon (NY) wedges that have a softer interaction with the surface of the reinforcement. The application of a thin layer of Epoxy (EP) coating was also investigated for additional protection during pulling.

The choice to investigate a range of material system and the progression from one system to another was motivated by technological as well as practical reasons. A VE-GFRP strand was investigated at an exploratory stage to validate the soundness of the concept. The system was improved by replacing traditional VE resin with innovative TP resin that allowed for easier manufacturing of complex twisted shapes. The development and calibration of a performing TP resin formulation required extensive investigation and lead to the development of a 12-mm bendable TP-GFRP bar as an intermediate step toward the development of a twisted strand. Meanwhile, 12.7-mm and 15.9-mm VE-GFRP bars have been characterized and investigated as a market-ready solution for mild and partial prestressing in some applications. The 15.2-mm twisted VE-GFRP and TP-GFRP strands have been developed at a prototypical stage and an industrial production line was set up by SIREG. The 12-mm TP-GFRP bar is ready for commercialization. The 15.9-mm VE-GFRP bar is market-ready and was deployed in mild-prestressed sheet piles in laboratory conditions at the University of Houston. The 12.7-mm VE-GFRP bar is market ready and was field-deployed in GFRP-partially-prestressed piles for a commercial project at the 23rd Avenue Bridge over Ibis Waterway managed by the Florida Department of Transportation.

CONCEPT AND INNOVATION

The state-of-the-practice with prestressing reinforcement identifies durability as the limiting factor for traditional High Strength Carbon Steel (HSCS) strands. Conversely, corrosion-resistant reinforcement solutions present constructability challenges and high material costs. Mild Prestressed Concrete (MPC) with GFRP tendons (GFRP-MPC) is proposed as an alternative approach that may allow overcoming some of these challenges. GFRP-MPC is meant for: a) pre-tensioning applications so that the anchor engages the strand only for a limited time and on a portion of the tendon that will not contribute to the strength of the PC element once completed; and, b) PC elements that require a limited level of prestress, are exposed to aggressive environments, and are not subjected to severe cyclic fatigue loading. These include piles, sheet piles, pile caps, and other elements of the bridge substructure. Precast and prestressed deck panels may also be an application in regions where deicing salts are used. The fundamental feature of GFRP-MPC consists in limiting the level of prestress at about 40% of the guaranteed tensile strength of the tendon. This value is set as a target required to achieve effective mild prestressing of substructure elements while guaranteeing adequate safety against failures due to pulling and creep-rupture. This choice results in a number of advantages when applied to a mechanically- and cost-efficient material:

1. Constructability considerations.

    a. Allows coupling the tendon to simpler and shorter anchors than the ones historically used for FRPs. Higher pull stresses would cause failures during pulling if ad-hoc anchors are not deployed. The ability to couple FRP tendons with traditional steel anchors that are available at any precast yard plays a critical role in easing constructability.

b. Prevents the splitting of concrete at tendon release as a consequence of pseudo-Poisson effect [3]. The splitting of concrete is a localized effect and can be restrained by adding transverse reinforcement. However, the reinforcement layout of typical PC members tends to be congested and additional reinforcement is not always an option. Furthermore: a) the confining capacity of FRP transverse reinforcement is limited by its relatively low modulus of elasticity; and, b) manufacturing of bent shapes is still a technological challenge.
c. The relatively high strain and the low modulus of elasticity of GFRP tendons represent appealing features during pre-tensioning operations. They allow for elongations during pulling similar to those of steel tendons even under lower levels of force.
d. To be efficiently deployed in prestressing applications at the industrial scale, a tendon should be coilable, shippable in long lengths, and cuttable to length as needed at the precast yard. The reduced elastic modulus and the larger guaranteed strain of GFRP ease coilability.

2. Tendons and PC elements performance.

a. A safe value of sustained pull at approximately 40% of the guaranteed tensile strength may be possible in GFRP-MPC based on recent experimental results on the creep-rupture performance of GFRP bars [1] and experiences with similar material systems [4].
b. The durability of GFRP has been addressed through the adoption of ECR glass fibers and vinyl-ester resin that meet the durability requirements of ASTM D7957M [5]. Experimental evidence was provided by Benmokrane et al. [6] for GFRP reinforcing bars. Stress corrosion can be a concern for tendons subject to sustained loads in aggressive environments. To account for the influence of environmental degradation on the creep-rupture performance of FRP reinforcement, an environmental knock down factor is applied to the creep-rupture strength of the material, as it is applied to its guaranteed strength for flexural strength calculations. The approach is traditional [7] and has been confirmed in recent design guidelines for FRP material systems in prestressing application [8].
c. Prestress losses are the product of concrete deformations – that are the sum of an elastic, a viscous, and a shrinkage component – multiplied by the stiffness of the tendon. With its relatively low modulus of elasticity, GFRP allows to retain a higher portion of the prestress initially applied with respect to stiffer materials such as HSCS and CFRP. Similar considerations date back to the first investigations into GFRP-RC/PC [9] and have been confirmed by more recent studies [4]. Relaxation – that is solely a function of the viscous properties of the reinforcement – also contributes to prestress losses but is typically the least relevant component in terms of magnitudes. Relaxation in GFRP material systems is reported to be only slightly higher with respect to CFRP and HSCS strands [10].
d. A relatively ductile behavior is one appealing feature of traditional HSCS tendons. GFRP tendons feature linear elastic behavior up to failure that occurs at guaranteed strains of approximately 2.0%. Accounting for an initial pre-tensioning at approximately 40% of the guaranteed tensile strength, the remaining strain reserve exceeds the threshold of 0.5% set by current standards for conventional PC [11, 12]. Thus, the deformation experienced by a GFRP-MPC element may provide enough warning before collapse occurs.
e. The twisted geometry of traditional HSCS strands ensure ideal bond to the concrete in addition to coilability. Similar geometries have been successfully used in CFRP commercial applications. Iyer & Lampo [13] report development lengths for twisted GFRP tendons to be in line with the ones of traditional HSCS strands.

INVESTIGATION

PART 1: DEVELOPMENT AND TESTING OF VE-GFRP STRANDS

During the first part of the project, a GFRP strand was developed using thermosetting Vinyl Ester resin and produced in small quantities to validate the concept, verify manufacturing capabilities, and conduct an exploratory investigation. The reported material properties and mechanical performance are indicative of the potential of the technology but, given the limited length manufactured, should not be considered representative of the quality of industrial production. The full characterization of the material system is of secondary importance with respect to investigating the technological challenges related to pulling using traditional anchoring systems.

The complete list of specimens tested is reported in Table 1. A limited number of tensile tests (T) was conducted to determine the tensile strength ($f_{f,u}$) of the GFRP strand. Pull tests (P) were conducted to measure the pull strength of the GFRP strand coupled with traditional steel anchors under instantaneous stress ($f_{f,ji}$). Pseudo-creep-rupture (CR) and pseudo-creep (C) tests were conducted on the GFRP strand coupled with traditional steel anchors under sustained stress ($f_{f,js}$) for time durations comparable to pre-tensioning operation ($t_{failure}$). Runout times are indicated with a star (*). Pseudo-relaxation (R) tests were conducted to measure the load loss following anchor setting (f_{12h}/f_i) together with the influence of various pre-tensioning procedures including the application of preload (RP) for a certain amount of time ($t_{preload}$) and the application of re-pulling (RR). A limited number of transverse shear tests (S) was conducted to measure the transverse shear strength ($\tau_{f,u}$). A flexural test (F) was conducted to measure the deflection limit at which first damaging occurs (δ_F) to investigate the potential for coilability. A total of four different geometrical configurations were investigated by varying the number of wire twists per meter from 1.25 to 4.50 that proved to have minimal influence on mechanical properties.

Material Characterization

The strand is composed by seven wires with a nominal diameter of 5.1 mm each. The nominal diameter of the strand is 15.2 mm while the average measured diameter is 14.5 mm with a coefficient of variation (COV) equal to 4.1% measured over 13 specimens. The average effective area of the strand is 128 mm^2 with a COV equal to 3.7% measured according to ASTM D7205 subsection 11.2.5.1 [14] over 23 specimens. This corresponds to an average effective diameter equal to 12.8 mm. The average measured diameter of the strand is 4.6% smaller than the nominal diameter. Tensile tests (T) were conducted according to ASTM D7205 [14] but over a reduced free length of 450 mm (30 diameters). The average ultimate tensile strength measured is equal to 859 MPa with a COV equal to 1.0%. The guaranteed tensile strength, defined as the average minus three standard deviations [7], is equal to 834 MPa. The value is slightly lower than the minimum set by ASTM D7957 [5] at 844 MPa for straight M6 bars but is significantly higher than the minimum set at 653 for M16 bars. M6 bars are the closest to the diameter of the single wires, M16 bars are the closest to the diameter of the strand. The average modulus of elasticity is equal to 44.5 GPa with a COV equal to 2.4%. The value is slightly lower than the minimum set by ASTM D7957 [5] at 44.8 GPa for straight bars of any diameter. The guaranteed strain is equal to 1.9%. Transverse shear tests (S) were conducted according to ASTM D7617 [15]. The average transverse shear strength measured is equal to 163 MPa with a COV equal to 4.2%. The guaranteed transverse shear strength is equal to 142 MPa. The value is higher than the minimum set by ASTM D7957 [5] at 131 MPa for straight bars of any diameter. Shear lag is known to reduce the guaranteed tensile strength at increasing bar diameter. Lumping together smaller-size wires to create a twisted strand allows achieving M6-like performance with a 15.2 mm diameter strand. However, twisting reduces the contribution of the fibers in the longitudinal direction determining lower values of elastic modulus and tensile strength without apparently affecting transversal properties.

Pull Strength Under Instantaneous Load

The test setup utilized is consistent with ACI 440.3R subsection B.10 [16] with conventional steel anchors applied to both ends of the specimen (Figure 3). The free length is 900 mm (60 diameters). The goal of this experiment is to determine whether the failure of the GFRP-anchor system happens at a load level that allows sufficient stressing of the GFRP strand. Pull tests (P) were conducted up to failure. Results are reported in Table 1. An average pull strength under instantaneous load equal to 524 MPa was measured with a COV equal to 3.8%. The guaranteed pull strength under instantaneous load, computed as the average minus three standard deviations, is equal to 464 MPa corresponding to 56% of the guaranteed tensile strength of the GFRP strand. The value meets the selected target and should be considered indicative of the potential of the technology. Figure 4a shows the load-displacement diagrams for four strands representative of each of the geometrical configuration considered. The displacement was measured at the cross-heads and is inclusive of the slipping between the strand and the anchors at the two ends. A strain hardening behavior can be observed as the wedges dig into the GFRP surface and gripping improves. Figure 4b shows the statistical distribution of the results of the pull tests. Even if the data set is limited, the results align along a Gaussian distribution (represented by the black line) confirming that the quantity measured is a stable property of the strand-anchor system and can be analyzed using the usual statistical assumptions.

Pull Strength Under Sustained Load

The strand-anchor system is required to maintain a certain level of sustained pull load for an estimated 12 hours. The system will undergo a creep-like phenomenon with the wedges slowly digging into the GFRP strand and slowly slipping under sustained load. The target in terms of guaranteed pull strength under a 12-hour sustained load is set at approximately 40% of the guaranteed tensile strength, a value deemed sufficient to achieve an effective prestressing design. Using the same set-up of the instantaneous test, a total of six tests were conducted allowing to record two failure points (labeled as pseudo-creep-rupture) and four runout points (labeled as pseudo-creep) interrupted at different times. Once the pre-set load level was reached, the load was maintained constant on the strand-anchor system until failure or runout time. In field pre-casting, the strand-anchor system is subject to a load that decreases over time as sitting losses occur; thus, the experimental setup is more demanding. Results of the pseudo-creep (C) and pseudo-creep-rupture (CR) tests are reported in Table 1. Failure points and runout points are reported in Figure 5a. Times to failure and times to runout are read on the x axis. Sustained pull forces are read on the y axis. A mean pseudo-creep-rupture function can be defined in as the dotted line shown in Figure 5a. To account for the variability in pull strength one can translate the curve down by a quantity equal to three standard deviations. The approach is in line with the work of Budelmann & Rostasy [17] and implies that the variability in pull strength remains constant over time. The 12-hour guaranteed pull strength threshold is shown as a black continuous horizontal line in Figure 5a. The limit is confirmed by four runout points reported as round dots with a horizontal arrow in Figure 5a. The 12-hour guaranteed pull strength meet the target set at approximately 40% GTS.

Pseudo-creep Behavior During Pull

The pseudo-creep behavior of the strand-anchor system was monitored and is shown in Figure 5b for 4 specimens representatives of each of the configurations tested. The displacement is plotted as a ratio with respect to the initial value recorded at the end of the loading ramp. The behavior is consistent with an average 12-hour displacement ratio equal to 1.11 with a COV equal to 1.2%. The displacement shown in Figure 5b was measured at the frame cross-heads and includes the creep deformation occurring within the GFRP strand, plus the slipping occurring between the anchor and the strand. To appreciate the significance of each contribution, one of the specimens (STR #1.50-CR) was instrumented with a 100 mm extensometer located at mid-length for the first half hour of testing. The results are shown in Figure 6. The extensometer is representative of the creep deformation occurring within the GFRP strand. The ratio of the loss related to GFRP creep with respect to the total displacement measured at the frame cross-heads at half hour is equal to 0.19.

The measure confirms how the creep behavior of the GFRP strand only accounts for a relatively small portion of the damage propagation that results in the pseudo-creep-rupture of the anchor-strand system. The main contribution is provided by the wedges of the anchor digging into the GFRP material and slowly slipping. Furthermore, shear lag at the anchors' location promotes stress concentrations on the external wires that are in direct contact with the wedges and prevents the load from being uniformly distributed over the effective area of the strand. This exacerbates damage propagation on the external wires that are the ones that eventually fail. The issue is acknowledged from historical references [18]. However, it is a necessary trade-off that allows to deploy an anchoring system that is optimal from the constructability standpoint. Traditional steel anchors coupled with GFRP strands are not able to provide the same level of performances achieved with HSCS strands (i.e. pull strength of approximately 75% of the ultimate tensile strength). However, they can guarantee performance that are deemed sufficient for an effective deployment in MPC applications.

Load Loss During Anchor Setting

As the wedges of the anchor engage the GFRP strand setting occurs, and load loss follows. Furthermore, some relaxation occurs within the GFRP strand. Such loss needs to be limited so that the load retained at the time of releasing (12 hours) is sufficient to meet design requirements. The phenomenon is labelled as pseudo-relaxation. A total of 10 pseudo-relaxation tests have been conducted using different pulling procedures. The test setup is consistent with ACI 440.3R subsection B.10 [16] but with anchors applied to both ends of the specimen. After the initial pulling, the total displacement is maintained constant on the strand-anchor system until a test duration of 12 hours is reached. The setup is representative of the actual conditions during pre-casting when the anchor lays against the stressing abutments and is prevented from moving. The imposed initial pull is equal to 348 MPa corresponding to 42% of the guaranteed tensile strength of the GFRP strand. The free length is equal to 900 mm.

A total of four pseudo-relaxation tests (R) have been conducted. Results are reported in Table 1. In Figure 7a the ratio of the retained pull at time *t* over the initial value is plotted for the four specimens tested. The behavior is consistent with an average 12-hour loss equal to 0.20 of the initial pull with a COV equal to 11.7%. The COV recorded for load loss is higher than the value recorded for pseudo-creep displacements because the quantity compared are one order of magnitude smaller, and the relative difference raises, therefore. However, the dispersions in term of absolute values (i.e. standard deviations) are comparable being 0.01 and 0.02 respectively. The load losses reported in Figure 7a include a component related to the slipping between strand and anchors that results in the elastic shortening of the strand, plus a relaxation component that occurs within the GFRP strand. To appreciate the entity of each contribution, one of the specimens (STR #1.50-R) was instrumented with a 100 mm extensometer located at mid-length for the first half hour of testing. The results are shown in Figure 7b. The extensometer is representative of the elastic shortening of the strand that is directly proportional to the load loss caused by slipping. The ratio of the extensometer measure to the total loss is equal to 0.49; thus, slipping accounts for about half of the total loss.

The contribution of slipping is significant but not predominant as it was in the case of pseudo-creep. Furthermore, the shortening of the strand following slipping at the anchors' location relieves the strand of some of the imposed displacement, thus reducing the severity of relaxation occurring within the strand as compared to a perfectly fixed case. The significance of the slip is constant at varying length of the strand. However, the relieving strain associated with the slip reduces at increasing length. Therefore, on longer strands, the influence of internal relaxation is expected to increase in relative terms whereas the contribution of the anchors reduces. This implies that a sustained load condition imposes additional burden on the interface between wedge and strand when compared to a more realistic sustained displacement condition. Nonetheless, the behavior reported in Figure 7b is only representative of the pseudo-relaxation performances of the strand-anchor system and not of the GFRP strand in service conditions for which values of approximately 2% of the guaranteed strength at 1-million-hour are reported in literature for a similar material system [10]. The average 12-hour load loss corresponds to 8.3% of the guaranteed tensile strength of the GFRP strand.

Influence of Twist per Meter

The dispersion of some of the measured quantities have been investigated at varying twist per meter. Figure 8a shows how the effective area of the GFRP strand remains stable. This validates the use of the same effective area for stress computations across different specimens. Similarly, Figure 8b shows how the pull strength of the GFRP strand remain stable. This supports the lumping together of measures of jacking strength and load loss performed on strands of different twist. The twisting may have an influence on other properties of the GFRP strand including its flexural properties and its bond performance that have not been investigated in this study.

Flexural Behavior and Coilability

Traditional HSCS strands and the relatively newer CFRP strands, are coiled around steel or wooden reels for storage. This allows them to overcome the length limitations imposed by straight bars that cannot be shipped at extents longer than 12 meters. To verify that the GFRP strand considered in this study can achieve similar bendability characteristics, one flexural test has been conducted on a specimen with a twist of 1.50 per meter. The strand is tested in a three-point-bending configuration in displacement control over a free span of 610 mm (40 diameters) as shown in Figure 9. Given the composite, orthotropic, and asymmetric nature of GFRP as a material system, to determine the flexural stiffness and the flexural strength of a round bar is a challenge from both the testing and modelling perspective [19]. The twisted geometry of a GFRP strand adds complexity. However, assuming that the flexural behavior is predominant over the shearing contribution, it is possible to compute the limit curvature of the GFRP strand based on a simple deflection measure [20]. The limit displacement at which the specimen shows the first damaging is 41 mm. The limit radius of curvature can be computed as the inverse of the limit curvature. This multiplied by two gives 1505 mm corresponding to the minimum diameter of the reel around which the strand can be coiled without damaging.

Partial Conclusions

This section of the report presents the results of an experimental investigation into GFRP strands for pre-tensioning applications. The study is conducted on a material system at the prototypical stage. Thus, results should be considered indicative of the potential of the technology, but not representative of industrial grade manufacturing and quality control. Specific findings are listed below.

1. The 7-wire GFRP strand has nominal diameter of 15.2 mm with an effective area of 128 mm^2, a guaranteed tensile strength of 834 MPa, and an average modulus of elasticity of 44.5 GPa.
2. The pull in the GFRP strand must be limited at approximately 40% of the guaranteed tensile strength of the GFRP strand to prevent creep-rupture over approximately 100 years of service life. The threshold is estimated from archival literature and previous experiences with similar material systems [1, 4].
3. The guaranteed pull strength of the GFRP strand coupled with traditional steel anchors under instantaneous load is measured at 56% of the guaranteed tensile strength of the GFRP strand alone. The value reduces when the strand-anchor system is engaged by a sustained load during pre-casting operations.
4. The guaranteed pull strength of the GFRP strand coupled with traditional steel anchors under a 12-hour sustained load is measured at 41% of the guaranteed tensile strength of the GFRP strand alone. The 40% target is met. Twelve hours correspond approximately to the period required for concrete to harden before releasing of the strands at the PC yard.
5. The average load losses during anchor setting settle at 8.3% of the guaranteed tensile strength of the GFRP strand.
6. The flexural properties of the GFRP strand have been investigated and coilability is possible around reels of approximately 1.5 m diameter. Coilability is critical to allow storage and shipping of the GFRP strand.

PART 2: DEVELOPMENT AND TESTING OF TP-GFRP REINFORCEMENT

The second part of the project focused on the development of GFRP reinforcement made with ECR glass fibers and TP resin in the form of a 5-mm wire, a 15.2-mm twisted strand, and a 12-mm coilable bar (Figure 10). The acrylic resin used in this study is an innovative compound specifically developed in a TP liquid form for composite applications by Arkema [21]. It features mechanical performances comparable to state-of-the-practice thermosetting VE resins typically used in GFRP bars manufacturing, plus the features of a TP resin in terms of workability and thermoformability. The mechanical properties of ECR fibers and TP resin used in this study are reported in Table 2 as the median values reported by OC (2010) and Becker et al. (2016). Furthermore, the properties of the TP-GFRP material systems developed in this study are reported in Table 2 as defined and extrapolated in the following sections of this report. Quantities reported include: tensile strength (f_{fu}), tensile modulus (E_f), tensile strain at rupture (ε_{fu}), transverse shear strength (τ_{fu}), interlaminar shear strength (η_{fu}), and limit elastic curvature (χ_{fu}). The material specifications set by ASTM D7957 [5] for a 6-mm bar are used as target for material development. The standard does not provide a minimum value for the interlaminar shear strength. Instead, the average strength of a VE-GFRP 6-mm bar from the same manufacturer is used as reference but does not represent a limit for acceptance. Furthermore, a limit curvature corresponding to the minimum required to guarantee coilability around a standard reel of 610-mm diameter per ASTM A416 [22] is used as target for flexural performance.

Thermoplastic GFRP Wire

The first attempt at developing TP-GFRP material systems focused on 5-mm wires to be later twisted to manufacture a strand for prestressing applications. Several production batches were progressively developed and tested to assess performances. Testing results are reported in Figure 11 as a ratio of the measured average to the respective target reported in Table 2 Each production batch is labelled "W" for wire and numbered progressively. The last two digits refer to the fiber content in terms of ratio to the total weight. The resin used is the same TP acrylic for all the batches. The composition differs slightly in terms of fillers and additives. Other differences include production speed, curing time, and fiber content. Macro groups can be defined as follows. Group 1 was manufactured on a small-scale pultrusion line for test purposes whereas from Group 2 onward an industrial-grade pultrusion line was developed. Group 3 marked a final refinement of the resin composition to improve bond and compatibility with ECR glass fibers.

The performances of the TP-GFRP wires tested improve at progressing production batch. Tensile modulus and transverse shear strength, mainly a function of the elastic properties of the fibers, have a similar development and easily meet the imposed target. Similarly, tensile strength and interlaminar shear strength, both dependent on the capacity of the resin to transfer stresses between the fibers, have a similar development but initially lay further from the imposed target. This suggested resin refinement was required. As the material system is improved, and the tensile test method is refined by using threaded steel tubes instead of laterally-gripped steel tubes, tensile properties improve with respect to interlaminar shear and lay half-way between interlaminar shear and transverse shear. Further details are provided in the following sub-sections. Eventually, production batch W-3.3/79 shows an average tensile strength of 891 MPa when tested using threaded steel tubes, an average transverse shear strength of 179 MPa, an average interlaminar shear strength of 14.2 MPa, and an average ultimate elastic curvature of 0.005 mm^{-1}.

Tensile Strength

Tensile tests were performed according to ASTM D7205 [14] over a free length of 590 mm. The tensile strength of TP-GFRP wires proved highly dependent on the type of anchoring adopted. Threaded steel tubes were eventually adopted in place of laterally-gripped steel tubes to minimize disturbances at the boundary and collect a representative measure of the performance of the material system. Both methods can be used interchangeably according to ASTM D7205 [14]. However, the thin diameter tested may be more sensitive to boundary disturbances with respect to the larger-diameter bars explicitly covered by the test method. Therefore, further refinement and adjustment were required. The evolution of average tensile strengths measured using the two different anchoring methods is shown in absolute terms in Figure 12 (left column: top). The statistical distribution of laterally-gripped tensile strength measurements in terms of Cumulative Distribution Function (CDF) is shown in Figure 12 (left column: center). The statistical distribution of laterally-gripped tensile strength measurements in terms of Gaussian Frequency Distribution Function (FDF) is shown in Figure 12 (left column: bottom). Moving from Group 1 to Group 3, the statistical distributions shift right toward higher averages and become thinner showing lower deviations as the material improves both in terms of average performance and consistency. Results with threaded steel tubes are limited and distributed over Group 1 and Group 2 not allowing to generate a statistic distribution. Data points are reported in Figure 12 (left column: top) and Figure 12 (left column: center) for reference.

Transverse Shear Strength

Transverse shear tests were performed according to ASTM D7617 [15]. In the test, a transverse blade cut through a laterally confined GFRP bar, rod, or wire with no free length between the supports and the blade. Lateral confinement keeps the specimen together even as interlaminar failure occurs. Therefore, transverse shear strength is expected to be higher with respect to interlaminar shear strength and mostly dependent on the properties of the fibers that keep resisting to transverse cutting even when interlaminar stress transfer through the resin has failed. The transverse shear test typically yields repeatable results and is commonly used as a standardized method for acceptance. A typical GFRP-TP wire tested in transverse shear is shown in Figure 13 (left). The evolution of average transverse shear strengths at varying production batch is shown in absolute terms in Figure 12 (central column: top). Statistical distributions are shown in Figure 12 (central column: center) in terms of CDF and in Figure 12 (central column: bottom) in terms of Gaussian FDF. Similar trends with respect to tensile strength distributions can be observed.

Interlaminar Shear Strength

Interlaminar shear tests, also called apparent horizontal shear tests, were performed according to ASTM D4475 [23]. The test resembles a three-point flexural test performed on a short span equal to 3 to 6 times the diameter of the bar, wire, or rod tested. In this study, a free length of 35 mm was selected as the minimum required to fit supports and allow loading procedures. The supports and loading apparatus for interlaminar shear testing provide a lower degree of confinement with respect to transverse shear testing. Therefore, the specimen fails when the capacity of the resin to transfer stresses interlaminarily is reached. A typical failure is shown in Figure 13 (right) with a crack opening in the longitudinal, or horizontal, direction that is the weakest for shear. Interlaminar shear tests performed on GFRP bars, wires, and rods are highly sensitive to the test setup adopted and the free span selected [23]. Interlaminar shear testing may yield less-repeatable results with respect to transverse shear testing. For this reason, interlaminar shear strength is typically not used as a requirement for acceptance [5]. Nevertheless, the test is a valuable resource from a research and development perspective to understand the behavior of a material system and the compatibility between its constituents. The relatively low value of interlaminar shear strength reported in Table 2 may be an inherent property of the type of resin or a biased result disproportionally affected by the small diameter tested and by the relatively long span adopted. The evolution of average interlaminar shear strengths at varying production batch is shown in absolute terms in Figure 12 (right column: top). Statistical distributions are shown in Figure 12 (right column: center) in terms of CDF and in Figure 12 (right column: bottom) in terms of Gaussian FDF. Similar trends with respect to tensile strength distributions can be observed.

Flexural Deformability

Flexural tests were performed according to ASTM D4476 [25] using the entire cross section of the wire over a free length of 270 mm. Load-curvature diagrams are plotted in Figure 14 for batch W-3.3/79. Two of the tests were performed in a 3-point-bending configuration and two in a 4-point bending configuration. An ultimate elastic curvature of 0.003 mm^{-1} guarantees coilability around a standard 610-mm reel per ASTM A416 [22].

Microscopy

Microscopical observation of the cross sections of TP-GFRP wire samples extracted from Group 1, Group 2, and Group 3 are shown in Figure 15 (left), Figure 15 (center), and Figure 15 (right) respectively. The porosity of the material reduces progressively in line with the progressive improvement of mechanical performance. The microstructure observed is not representative of the quality of a large-scale industrial production. However, it is deemed sufficient at an exploratory stage and its evolution confirms the mechanical trends previously observed.

Fiber Content, Cross Section, and Microscopy

Fiber content by volume was measured according to ISO 1172 [26] on selected production batches registering an average difference of 2.2% with respect to the value set during manufacturing. The latter is reported for every production batch in this study. Cross sectional area was measured according to ASTM D7205 [14] on selected production batches registering an average error of 1.1% with respect to the value computed using the average diameter measured with a caliber. The latter was used to compute the stresses reported in this study.

Thermoplastic GFRP Strand

Prestressing strands are made of multiple wires combined in a twisted shape. Both for the case of steel and FRP, the strand is expected to retain most of the properties of the single wire in terms of strength and flexibility. Rossini & Nanni [20] reported an average tensile strength of 859 MPa for twisted VE-GFRP strand corresponding to 98.8% of the average tensile strength of a 6-mm VE-GFRP bar from the same manufacturer. A similar reduction may be expected in moving from a 5-mm TP-GFRP wire from production batch W-3.3/79 to a 15.2-mm twisted strand for which a tensile strength of 881 MPa can be extrapolated. A limited number of such strands were manufactured for exploratory purposes. Manufacturing involved reheating and thermoforming to give the material system its twisted and helical shape.

Testing was performed on available material prioritizing the assessment of its compatibility with traditional pre-tensioning steel anchoring systems. Pull tests were performed according to ACI 440.3R subsection B.10 [16] applying pre-tensioning anchors at both ends of the strand. A detail of an anchored strand ready for testing is shown in Figure 16 (left). A thin layer of epoxy coating (EP) was applied on the gripped portion of the strand. This solution allowed to achieve performances comparable to the VE-GFRP strands tested by Rossini & Nanni [20]. Results are reported in Figure 16 (right) plotting stresses against slippage occurring at the anchor location. Slippage associated to a single anchor is measured subtracting the elastic deformation to the total cross-head movement and dividing the value by two. The average tensile modulus is measured as 45.6 GPa applying a 100-mm extensometer that was removed before failure occurred. Testing without epoxy coating proved unfeasible because of excessive slippage at the anchor location making it difficult for the steel anchors to grip and for load to build up.

Thermoplastic GFRP Bar

The development of TP-GFRP reinforcing bars may have potential implications on reinforcement, manufacturing, bendability and may allow a reorganization of the supply chain. Furthermore, the development of a 12-mm TP-GFRP bar may offset some of the scale challenges experienced while working with 5-mm TP-GFRP wires. A sample batch was produced and tensile tested according to ASTM D7205 [14] showing an average tensile strength of 948 MPa and an average tensile modulus of 48.0 GPa over a measured area of 116 mm^2. To explore the possibility of bending through thermoforming, a small-scale sample was post-heated, bent at a diameter of 40 mm, and tested using a setup similar to the pullout test regulated by ASTM D7913 [24] and shown in Figure 17 (left). The performance of the TP-GFRP bent tested align to VE-GFRP bents from the same manufacturer as shown in Figure 17 (right). However, larger scale testing on a wider range of bent diameters should be performed to fully assess this property.

Partial Conclusions

The second part of the project investigates the challenges and opportunities related to the development of GFRP reinforcement made with ECR fibers and TP resin in the form of a 5-mm wire, a 15.2-mm twisted strand, and a 12-mm coilable bar. The material systems investigated are not representative of a large-scale industrial production but were developed for exploratory purposes. After adequate development, TP-GFRP material systems proved able to provide satisfactory mechanical performances in terms of tensile strength, tensile modulus, transverse shear strength, and flexural deformability. The TP-GFRP 15.2-mm strands tested showed compatibility with traditional steel pre-tensioning systems provided that a thin epoxy coating is applied to guarantee additional protection. The opportunity offered by thermoformability and heating allowed manufacturing of complex shapes in the form of twisted strands and bent bars.

PART 3: COMPATIBILITY OF GFRP REINFORCEMENT WITH VARIOUS ANCHORING SYSTEMS

The third part of this project investigates the compatibility of GFRP material systems with various types of anchors. The nomenclature “XXX/YY/ZZ-type of test” is used through this section. Where: “XXX” describes the geometry of the material system, “YY” describes the type of constituent resin, “ZZ” describes the type of anchoring system. When necessary, details regarding the type of test performed on each specimen are provided after a dash. Table 3 summarized the mechanical properties of the five GFRP material systems investigated in this project in terms of mean cross sectional area (a_f), mean ultimate tensile strength (UTS) (f_{fu}), mean modulus of elasticity (E_f), mean ultimate tensile strain (ε_{fu}), mean transverse shear strength (η_{fu}), and mean ultimate elastic curvature (χ_{fu}) and corresponding minimum diameter of curvature (D_R). The five material systems are:

- STR/TP: a 7-wire 15.2-mm strand made of ECR glass fibers and TP resin developed in Part 2 of this project.
- M12/TP: a 12-mm coilable bar made of ECR glass fibers and TP resin developed in Part 2 of this project.
- STR/VE: a 7-wire 15.2-mm strand made of ECR glass fiber and VE resin developed in Part 1 of this project.
- M13/VE: a 12.7-mm coilable bar made of ECR glass fibers and VE resin [27].
- M16/VE: a 15.9-mm bar made of ECR glass fibers and VE resin [27].

The three anchoring systems considered are:

- ST: traditional steel pre-tensioning anchors shown in Figure 18 (top). Model “Paul F50B-38” is used for 15.2-mm strands and 15.9-mm bars and model “Paul F44B-30” is used for 12.7-mm bars [28].
- EP: a thin layer of epoxy coating applied to the surface of the reinforcement to improve contact with traditional ST anchors as shown in Figure 18 (center).
- NY: alternative pre-tensioning anchors using a steel barrel and polymeric Nylon wedges (NY) shown in Figure 18 (). Model SIREG Blocking System 50x85 TDS-518 is used for 12.7-mm bars [29].

Initial Pull strength

The test setup is consistent with ACI 440.3R subsection B.10 [16] with conventional steel anchors applied to both ends of the specimen. The goal of this experiment was to determine whether the failure of the GFRP-anchor system happens at a load level that allows sufficient stressing of the GFRP strand and to compare the performance of different material and anchor systems. Pull tests (P) were conducted up to failure. Results are reported in Table 4 in terms of mean pull strength ($f_{f,pi}$), guaranteed pull strength ($f_{f,pi}$*) computed as the mean value minus three standard deviations, coefficient of variation (COV), and mean slippage at failure measured by subtracting the elastic component to the total cross-head movement and dividing the quantity by the number of anchors (2). The performance of the different systems tested are shown in Figure 19 (left) in terms of pull load over total displacement, and in Figure 19 (right) in terms of pull stress over slippage at the anchor location. The material and anchor systems investigated are:

- STR/TP/ST: the TP strand developed in Part 2 of this project coupled with traditional Steel (ST) pre-tensioning anchor was not able to properly grip and build up strength because of excessive slippage at low level of stress.

- STR/TP/EP: the TP strand developed in Part 2 of this project protected with a thin Epoxy (EP) coating and coupled with ST anchors showed relevant slippage but was able to build up adequate pull strength. The curve shown in Figure 19 is an average of 2 repetitions.
- STR/VE/ST: the VE strand developed in Part 1 of this project coupled with traditional Steel (ST) pre-tensioning anchors showed limited slippage and the ability to build up adequate pull strength. The curve shown in Figure 19 is an average of 7 repetitions.
- M16/VE/ST: 15.9-mm VE bars coupled with traditional Steel (ST) pre-tensioning anchors showed limited slippage and good strength buildup. The higher value obtained in terms of pull force is related to the larger cross-sectional area rather than better coupling with the anchoring system. The curve shown in Figure 19 is an average of 5 repetitions.
- M13/VE/ST: 12.7-mm VE bars coupled with traditional Steel (ST) pre-tensioning anchors showed limited slippage and good strength buildup. The curve shown in Figure 19 is an average of 6 repetitions.
- M13/VE/NY: 12.7-mm VE bars coupled with an alternative anchoring system that uses a steel barrel and polymeric Nylon (NY) wedges showed the limited slippage and good strength buildup. The curve shown in Figure 19 is an average of 4 repetitions.

All the VE-GFRP systems showed a consistent behavior in terms of stresses with some variations in terms of slippage at the anchor location: the more regular the geometry of the reinforcement, the lower the slippage. Similarly, the more compatible the anchoring system in terms of surface thoughtless (NY vs ST), the lower the slippage. It may be inferred that the pull strength of a VE-GFRP material system is mostly a function of the transverse strength of the material that is not affected by the reinforcement size as for the case of tensile strengths. Therefore, a conservative approach can be adopted lumping together the data collected on STR/VE/ST, M16/VE/ST, M13/VE/ST, and M13/VE/NY to compute the average initial pull strength for VE-GFRP material systems as 581 MPa with a COV equal to 8.8% for a guaranteed initial pull strength of 428 MPa.

To support the approach adopted, statistical modelling was performed to verify whether the all VE-GFRP material systems can be lumped together in the same statistical distribution. Figure 20 (left) shows how the measured quantities align to an ideal normal Cumulative Distribution Function (CDF). Similarly, Figure 20 (right) shows how the data collected align to an ideal normal Frequency Distribution Function (FDF). Statistical testing was performed according to the Kolmogorov-Smirnoff method and the goodness-of-fit method. Both approaches show adherence to the model at a significance level higher than 25%. A significance level of 5% is conventionally considered a threshold for acceptance.

Pseudo-creep tests

Pseudo-creep tests were conducted on STR/VE/ST (4 repetitions), M16/VE/ST (3 repetitions), and M13/VE/ST (3 repetitions) to evaluate the ability to maintain a sustained pull for a minimum of 12-hours and measure the slippage occurring at the anchor location measured as the ratio of the final to the initial displacement and in terms of delta variation. The same setup as for initial pull strength tests was adopted maintaining the load constant for the entire duration of the test, after reaching the desired value. The level of stresses and mean test results for each material-anchor system are reported in Table 5. Average curves are plotted in Figure 21. Results confirm how more regular cross sections undergo less slippage at the anchor location.

Pseudo relaxation tests

Pseudo-relaxation tests were conducted on STR/VE/ST (4 repetitions), M16/VE/ST (1 repetition), and M13/VE/NY (3 repetitions) to evaluate the ability to maintain a sustained displacement for a minimum of 12-hours and measure the related load loss. The same setup as for initial pull strength tests was adopted maintaining the displacement constant for the entire duration of the test, after reaching the desire value. The level of stresses and mean test results for each material-anchor system are reported in Table 6. Average curves are plotted in Figure 22. Results confirm how more regular cross sections undergo less slippage at anchor location. The use of more compatible and softer NY wedges has a significant effect in reducing load losses. Seating losses at a precast yard are estimated considering that approximately 50% of the measured losses are related to slipping and a function of the length of the specimen tested whereas the rest is an inherent relaxation phenomena occurring, without slippage, either within the tendon, within the anchor, or at the tendon-anchor interface as shown using extensometer measurements in Part 1 of this project. Alternative pull procedures have been investigated as discussed in the following subsections to evaluate their effect on load losses. A summary of the results and test parameters is reported in Table 6.

Pseudo-relaxation tests with preload

Four specimens have been subjected to a preload equal to the initial pull for a certain period of time before being engaged in displacement control. The test is labelled pseudo-Relaxation with Preload (RP). The preload durations selected are 1 minute, 5 minutes, 10 minutes, and 15 minutes. Results are reported in Table 6. Figure 23 (left) shows the development of load losses in specimens subjected to different preload durations. Losses consistently reduces at increasing preload duration. Furthermore, Figure 23 (right) shows how the 12-hour load losses decrease with a linear trend at increasing preload duration. The R^2 is 0.97. The results are aligned to the expected mechanical behavior: to maintain a sustained preload applied on the strand allows the wedges of the anchor to grip into the material and GFRP relaxation to exhaust while load losses are compensated. The total load loss is reduced to 0.10 of the initial pull by applying a 15-minute preload. However, to maintain a sustained preload during pre-tensioning operations may represent a challenge.

Pseudo-relaxation tests with re-pull

A total of four specimens have been re-pulled after 20 minutes (1 repetition), 60 minutes (1 repetition), and 720 minutes or 12 hours (2 repetition) from the initial pull. The anchors are maintained in the same location. This allows for the wedges to develop optimal gripping during the pseudo-relaxation after the first pull and for the GFRP inherent relaxation to be exhausted as well. The test is labelled pseudo-Relaxation with Re-pull (RR). Results are reported in Table 6. Pseudo-relaxation curves are shown in Figure 24 (left). Figure 24 (right) shows that the load losses at 12 hours decrease in a non-linear fashion suggesting that re-pulls performed shortly after the initial pull may be a more efficient solution rather than leaving the material-anchor system seating overnight. Re-pulling has been historically performed on HSCS strands before the development of low-relaxation alloys. Thus, it is a procedure that many precasters are familiar with.

Pseudo-relaxation tests with multiple re-pulls

Finally, it was tested whether a higher number of shorter (20 minutes) re-pulls would yield a positive effect on the pseudo-relaxation performance of the material-anchor system. Table 6 and Figure 25 show how a single pull has positive effects on reducing load losses, whether increasing the number to two pulls may damage the interface between anchor and GFRP reinforcement, yield no additional reduction no load losses, and potentially have detrimental effects on the overall mechanical performance of the material.

Pull Strength Under Sustained Load

A total of 3 pseudo-creep-rupture points, 11 runout points in pseudo-creep loading conditions, and 19 runout points in pseudo-relaxation loading conditions have been collected on VE-GFRP material systems as shown in Figure 26. By interpolating the pseudo-creep-rupture points, it is possible to extrapolate the mean pull strength under sustained load at 12 hours as 379 MPa. By shifting the curve down by three standard deviations, it is possible to define a guaranteed pull strength under sustained load as 226 MPa. Figure 26 shows how this value is a very conservative estimation that lays far below the actual rupture points and runout points measured and collected.

Partial Conclusions

In the third part of the study the pull performance of 4 different material systems coupled with 3 different anchoring system were evaluated in terms of initial pull strength, sustained pull strength, and seating losses. Specific considerations are reported below:

1. Strands made with ThermoPlastic resin (STR/TP) were tested using traditional Steel (ST) anchors and applying a thin layer of Epoxy (EP) coating. The latter yielded adequate initial pull strength performance. However, limited data are available for further extrapolation at this stage.
2. The statistical analysis of initial pull strength results of reinforcement made with Vinyl Ester resin (STR/VE, M16/VE, M13/VE, M13/NY) supports the position that the pull performance of these material system is mainly a function of the transverse and surface properties of the resin and is affected to a lesser degree by the geometry of the reinforcement and the type of anchor used.
3. The type of anchor has a relevant influence on seating losses experienced during pull. The more compatible the anchor system (NY vs ST) and the more regular the surface of the reinforcement (M13 vs STR), the lower seating losses. The use of M13/VE bars coupled with anchors with polymeric Nylon (NY) wedges delivers optimal performances among the tested alternative and is considered the most suited option for field deployment at the current stage.
4. The mean initial pull strength of VE-GFRP material systems can be estimated as 581 MPa with an 8.8% COV resulting in a guaranteed initial pull strength of 428 MPa corresponding to 58% of the Guaranteed Tensile Strength (GTS) of M13/VE bars per ASTM D7957 [5].
5. The mean sustained pull strength of VE-GFRP material systems can be estimated through extrapolation in a logarithmic diagram as 379 MPa at 12 hours, corresponding to a guaranteed sustained pull strength of 226 MPa at 12 hours. This corresponds to 30% GTS for M13/VE bars per ASTM D7957 [5]. This is a low-bound very conservative estimate as shown by runout points reported in Figure 26.
6. Using M13/VE bars coupled with polymeric NY wedges, seating losses at a precast yard can be estimated as approximately 5% of the initial pull. Other material and anchoring systems typically show higher seating losses.

PART 4: LONG-TERM CREEP RUPTURE STRENGTH OF GFRP REINFORCEMENT

In an effort synergetic to MILDGLASS, the authors contributed to the evaluation of the creep-rupture strength of GFRP bars. A large database of historic and recent data was collected and published by Benmokrane, Brown, Mohamed, Nanni, Rossini, and Shield [1]. Meanwhile, Rossini, Saqan, and Nanni [2] investigated additional data and developed a novel method of analysis based on statistical considerations. In Figure 27 the method developed by Rossini, Saqan, and Nanni. [2] is applied to a comprehensive databased of 195 creep-rupture points and 42 runout points to evaluate a guaranteed value of creep-rupture strength for VE-GFRP reinforcement. The characteristic curve is rotated and shifted to account for existing variabilities along both the time and load axes. The guaranteed curve is shifted lower down for additional safety in line with the provisions of ACI 440.1R [7], and Eurocode 0 [30]. Runout points do not affect the analysis and are only reported for reference. The database includes a range of bar sizes from 9-mm to 20-mm from 7 different manufacturers. For additional information on the method of analysis, refer to the published references mentioned above.

The method yields a guaranteed creep-rupture strength for VE-GFRP reinforcement at 114 years equal to 42% GTS. The value is higher than the target set as 40% GTS in Part 1 of this report and higher than the level of pull to be applied on M13/VE according to Part 3 of this study. Therefore, creep-rupture is not a limiting factor for VE-GFRP prestressing.

PART 5: STRUCTURAL TESTS ON GFRP-PRESTRESSED FLEXURAL MEMBERS

Structural tests on GFRP-prestressed flexural members were conducted at the University of Houston (UH) by the research teams lead by Dr. Abdeldjelil Belarbi as part of a collaborative effort to MILDGLASS funded with a seed grant sponsored by the Hurricane Resilience Research Institute (HuRRI). Six full scale beams were built in three different configurations:

- Configuration A: prestressed with 16 M16/VE/ST with a target pull of 58 kN each.
- Configuration B: prestressed with 16 M13/VE/ST with a target pull of 44 kN each.
- Configuration C: prestressed with 8 M16/VE/ST with a target pull of 58 kN each.

Two repetitions for each configuration were produced and tested, except for configuration C. In that case one member was prestressed, while the other was not-prestressed and tested as baseline for comparison. During pulling some challenges were encountered in coupling M13/VE to traditional Steel (ST) anchors, further supporting the choice of using polymeric Nylon (NY) wedges in future applications as discussed in Part 3 of this report. For further information on structural testing refer to a report separately submitted to HuRRI by UH. Casting of the structural elements is shown in Figure 28. An extract from the conclusions of the UH-HuRRI report is reported verbatim:

"Based on what has been observed from the prestressing operations, M13 GFRP rebars can exhibit failure at chuck location during the pulling phase or in the following. This problem may be avoided if an industrial prestressing equipment is used, pulling all rebars at one time, by avoiding the repetitions of manual operations that may damage the bar (hammering of the chucks). GFRP rebars are not affected by significant creep or relaxation if the pre-stressing level is limited up to 45% of the ultimate. In conclusion, traditional prestressing equipment can be considered suitable to this orthotropic composite material. The mechanical tests have shown the brittle behavior at failure, caused by tensile rupture of the GFRP tendons. From the analysis of the experimental data, the test results look in good agreement with the analytical predictions."

PART 6: DEMONSTRATOR CONSTRUCTED AT 23RD AVENUE BRIDGE OVER IBIS WATERWAY

Two demonstrative piles partially-prestressed using coilable M13/VE bars have been constructed for installation at the FDOT-managed 23rd Avenue Bridge over Ibis Waterway in Broward County (FL). The piles have a cross section of 457x457 mm and are pre-tensioned using 12 M13/VE bars pulled at 30 kN after seating losses using NY anchors. The reinforcement includes 12 non-prestressed M25/VE bars and M13/VE closed-loop stirrups. Pre-casting operations are shown in Figure 2, the design of the piles is shown in Figure 29, and additional details are discussed in Appendix 2.

PART 7: ECONOMIC IMPLICATIONS AND LIFE CYCLE COST (LCC) ANALYSIS

The last component of this study quantified the economic implications of the technology, focusing on the structural configuration demonstrated in Part 6 of this report. Projections show how a GFRP partially prestressed pile may feature an initial cost at approximately two thirds of a CFRP- or HSSS-prestressed pile and a Life Cycle Cost (LCC) approximately 40% lower than a traditional pile prestressed using carbon steel strands. Details are provided in Appendix 2.

PLANS FOR IMPLEMENTATION

Several steps were undertaken to promote the dissemination of the findings of this study to transportation officials, bridge engineers, researchers, and members of the composite industry and leverage wider deployment of GFRP prestressing in transportation infrastructures. A detailed list of publications, presentations, communication efforts, and implementation initiatives is reported in Appendix 3. These efforts include:

- The MILDGLASS concept and project outcomes were presented in national and international venues including the 2020 TRB Annual Meeting, the 2019 IABSE Congress, the 2019 ACI fall convention, the 2019 BEI Conference, the 2018 CICE International Conference, the 2018 IHEEP Conference, the 2018 International *fib* Conference.
- The results of MILDGLASS and related efforts were published in scientific papers that appeared in national and international journals including: ACI, ASTM, CONMAT, JCC, SIE.
- MILDGLASS appears in the 2020 NCHRP-IDEA Report to the AASHTO Research and Innovation Committee and was awarded the 2019 JEC Innovation Award. These achievements highlight the interest in this technology expressed by both transportation officials and the composite industry.

FDOT, a key stake holder, is the first utilizer of the technology, potentially leading a nation-wide pre-standardization effort. The two partially-prestressed piles to be installed at the FDOT-managed 23rd Avenue Bridge over Ibis Waterway in Broward County (FL) serve as the first real-life demonstrator of the MILDGLASS concept. Discussion is underway with counties and local administrations in Florida to install mild-prestressed piles in seawall rehabilitation projects. Several industrial partners were involved in this project and maintain their commitment to leverage the diffusion of the technology. This includes SIREG as an FRP manufacturer, Arkema as a resin manufacturer, Owens Corning as a glass fiber and GFRP manufacturer, Gate Precast Company as a precaster, and Buzzi Unicem as a cement manufacturer and ready mix producer.

FINDINGS AND CONCLUSIONS

The project had a duration of 2 years and was subdivided into two stages. Stage I focused on the development, testing, and characterization of GFRP coilable material systems for concrete prestressing. Stage II focuses on the design, construction, and testing of demonstrative structures using pre-tensioned GFRP reinforcement. Of the four coilable material systems considered, M13 VE-GFRP coilable bars coupled with NY wedges proved ready for field deployment in pre-tensioning projects at a pull of 30 kN (233 MPa) after seating losses, corresponding to approximately 30% of the Guaranteed Tensile Strength (GTS) of the bar per ASTM D7957. The other material systems investigated showed promising performance in laboratory conditions and have been developed at a prototypical stage. Experimental testing of the four coilable GFRP material systems showed initial pull strengths ranging from 62 kN to 94 kN (452 MPa to 675 MPa) depending on the material system and the type of anchor considered. Displacement-controlled tests under sustained pull were performed to simulate the behavior of the reinforcement-anchor systems during pre-tensioning operations at a typical precast yard. Tests were conducted at different time durations ranging from 12 hours at 45 kN (348 MPa) on VE-GFRP strands to 7 days at 38 kN (294 MPa) on VE-GFRP M13 straight bars. Results showed compatibility with traditional pulling procedures. Specific findings are listed below:

1. The first part of the project focused on developing a VE-GFRP strands for pre-tensioning applications. This first step validated the feasibility of GFRP prestressing. The material system was developed at a prototypical stage and showed adequate mechanical performance for concrete mild pre-tensioning.
2. The second part of the project focused on developing a TP-GFRP strand and a TP-GFRP bar for pre-tensioning and reinforcement applications. The material systems were developed at the prototypical stage, after adequate refinement they showed adequate mechanical properties.
3. The third part of the project investigated the compatibility of VE-GFRP and TP-GFRP reinforcement with three different anchoring systems including traditional Steel (ST) anchors, the applications of Epoxy (EP) coating for additional protection, and the use of polymeric Nylon (NY) wedges.
4. The material and anchoring systems investigated in Part 1, Part 2, and Part 3 of this project all showed adequate or promising performance for deployment in pre-tensioning applications. The optimal solution at the current stage is to use coilable M13/VE bars coupled with anchors using polymeric Nylon (NY) wedges at an initial pull after seating losses of 30% of their Guaranteed Tensile Strength (GTS) per ASTM D7957 [5].
5. The fourth part of the project focused on assessing the guaranteed creep-rupture strength of VE-GFRP reinforcement that was estimated at 42% GTS performing statistical investigations over a database of 195 creep-rupture points and 42 runout points collected over diameters ranging from 9-mm to 20-mm and 7 different manufacturers. This confirms how long-term creep-rupture strength is not a limiting factor for GFRP prestressing.

6. The fifth part of the project focused on structural tests performed on VE-GFRP-prestressed flexural members. Test results confirmed adequate performances of the prestressed elements and highlighted some challenges related to the use of traditional Steel (ST) anchors coupled with M13/VE bars. This supports the use of NY anchors.
7. The sixth part of the project focused on designing, building, and installing two demonstrative piles partially-prestressed using coilable M13/VE bars pulled using NY anchors. The piles have been constructed for installation at the 23rd Avenue Bridge over Ibis Waterway in Broward County (FL). Construction of the bridge is underway.
8. The last component of this study quantified the economic implications of the technology, focusing on the structural configuration demonstrated in Part 6 of this report. Projections show how a GFRP partially prestressed pile may feature an initial cost at approximately two thirds of a CFRP- or HSSS-prestressed pile and a Life Cycle Cost (LCC) approximately 40% lower than a traditional pile prestressed using carbon steel strands.

Based on these findings, the following conclusions can be drawn:

- GFRP tendons can be effectively coupled with simple anchoring systems guaranteeing pull strengths and load losses that allow for the design of elements that require relatively low levels of prestress.
- The ability to couple GFRP tendons with simple anchors will minimize impact on traditional precasting operations.
- GFRP tendons provide a cost-effective non-corrosive alternative to traditional steel strands in applications that require relatively low levels of prestress and are located in aggressive and corrosive environments.

INVESTIGATORS' PROFILE

Antonio Nanni, Ph.D., P.E., F.ACI, F.ASCE, F.IIFC, F.BEI is the Inaugural Senior Scholar, Professor and Chair, in the Department of Civil, Architectural, and Environmental Engineering at the University of Miami, FL. He serves as Chair of ACI Committee 549. He serves as voting member of ACI Committee 440. His research interests include construction materials and their structural performance and field application.

Marco Rossini, Ph.D., M.Sc.Eng., Zegna Scholar, has been a research and teaching assistant at the University of Miami from August 2015 through December 2019 when he completed his PhD in structural engineering. Rossini is a member of ACI Committees 423 and 440. His research interests include structural performances of innovative materials for new construction and rehabilitation, and the development of rational design methods, guidelines, and codes.

REFERENCES

[1] Benmokrane, Brahim, Vicki L Brown, Khaled Mohamed, Antonio Nanni, Marco Rossini, and Carol Shield. "Creep-Rupture Limit for GFRP Bars Subjected to Sustained Loads." *Journal of Composites for Construction* 23, no. 6 (December 2019): 06019001(1-7).

[2] Rossini, Marco, Elias Saqan, and Antonio Nanni. "Prediction of the Creep Rupture Strength of GFRP Bars." *Construction and Building Materials* 227 (2019): 116620(1-11).

[3] Roddenberry, Michelle, Primus Mtenga, and Kunal Joshi. *Investigation of Carbon Fiber Composite Cables (CFCC) in Prestressed Concrete Piles*. Tallahassee, FL: Florida State University. Department of Civil and Environmental Engineering, 2014.

[4] Zawam, M., K. Soudki, and J.S. West. "Effect of Prestressing Level on the Time-Dependent Behavior of GFRP Prestressed Concrete Beams." *Journal of Composites for Construction* 21, no. 4 (2017): 1–10.

[5] ASTM. *Standard Specification for Solid Round Glass Fiber Reinforced Polymer Bars for Concrete Reinforcement. D7957/D7957M−17*. West Conshohocken, PA: ASTM International, 2017.

[6] Benmokrane, Brahim, Ahmed H. Ali, Hamdy M. Mohamed, Adel ElSafty, and Allan Manalo. "Laboratory Assessment and Durability Performance of Vinyl-Ester, Polyester, and Epoxy Glass-FRP Bars for Concrete Structures." *Composites Part B: Engineering* 114 (2017): 163–74.

[7] ACI Committee 440. *Guide for the Design and Construction of Structural Concrete Reinforced with Fiber-Reinforced Polymer (FRP) Bars. ACI 440.1R-15*. Farmington Hills, MI: American Concrete Institute, 2015.

[8] AASHTO. *LRFD Bridge Design Guide Specifications for GFRP-Reinforced Concrete*. 2nd ed. Washington, DC: American Association of State Highway and Transportation Officials, 2018.

[9] Wines, J C, and G C Hoff. *Laboratory Investigation of Plastic-Glass Fiber Reinforcement for Reinforced and Prestressed Concrete. Report 1: Plain Reinforced Concrete*. Vicksburg, MS: US Army Corp of Engineers Waterways Experiment Station, 1966.

[10] Wolff, R, and H J Miesseler. “Glass Fibre Prestressing System.” In *Fiber-Reinforced-Plastic (FRP) Reinforcement for Concrete Structures: Properties and Applications*, edited by Antonio Nanni, 1st ed., 305–32. Amsterdam, NL: Elsevier Science Publisher, 1993.
[11] ACI Committee 318. *Building Code Requirement for Structural Concrete and Commentary. ACI 318-14*. Farmington Hills, MI: American Concrete Institute, 2014.
[12] AASHTO. *LRFD Bridge Design Specifications*. 8th ed. Washington, DC: American Association of State Highway and Transportation Officials, 2017.
[13] Iyer, S L, and Richard G Lampo. *Demonstration of Advanced Composite Cables for Prestressing Applications in Concrete Waterfront Structures. USACERL Technical Report 98/33*. Washington, DC: US Army Corp of Engineers, 1998.
[14] ASTM. *Standard Test Method for Tensile Properties of Fiber Reinforced Polymer Matrix Composite Bars. D7205/D7205M−06*. West Conshohocken, PA: ASTM International, 2006.
[15] ASTM. *Standard Test Method for Transverse Shear Strength of Fiber-Reinforced Polymer Matrix Composite Bars. D7617/D7617M−11*. West Conshohocken, PA: ASTM International, 2011.
[16] ACI Committee 440. *Guide Test Methods for Fiber-Reinforced Polymer (FRP) Composites for Reinforcing or Strengthening Concrete and Masonry Structures. ACI 440.3R-12*. Farmington Hills, MI: American Concrete Institute, 2012.
[17] Budelmann, H, and F Rostasy. “Creep Rupture Behavior of FRP Elements for Prestressed Concrete: Phenomenon, Results and Forecast Models.” *ACI Special Publication* 138 (1993): 87–100.
[18] Erki, M A, and S H Rizkalla. “Anchorages for FRP Reinforcement.” *Concrete International* 15, no. 6 (1993): 54–59.
[19] Zhang, Burong, Radhouane Masmoudi, and Brahim Benmokrane. “New Method for Testing Fiber-Reinforced Polymer Rods Under Flexure.” *Journal of Testing and Evaluation* 35, no. 2 (2006): 171–76.
[20] Rossini, Marco, and Antonio Nanni. “Composite Strands for Prestressed Concrete: State-of-the-Practice and Experimental Investigation into Mild Prestressing with GFRP.” *Construction and Building Materials* 205 (2019): 486–98.
[21] Becker, David, Gilles Francois, Virginia Bozsal, and Peter Mitschang. “Combining the Best of Two Polymer Worlds.” *Kunststoffe International* 106, no. 12 (2016): 49–51.
[22] ASTM. *Specification for Low-Relaxation, Seven-Wire Steel Strand for Prestressed Concrete. ASTM A416/A416M−17*. West Conshohocken, PA: ASTM International, 2017.
[23] ASTM. *Standard Test Method for Apparent Horizontal Shear Strength of Pultruded Reinforced Plastic Rods by the Short-Beam Method. ASTM D4475-02(2016)*. West Conshohocken, PA: ASTM International, 2002.
[24] ASTM. *Standard Test Method for Bond Strength of Fiber-Reinforced Polymer Matrix Composite Bars to Concrete by Pullout Testing. D7913/D7913M-14*. West Conshohocken, PA: ASTM International, 2014.
[25] ASTM. *Standard Test Method for Flexural Properties of Fiber Reinforced Pultruded Plastic Rods. D4476/D4476M-14*. West Conshohocken, PA: ASTM International, 2014.
[26] ISO. *Textile-Glass-Reinforced Plastics - Prepregs, Moulding Compounds and Laminates - Determination of the Textile-Glass and Mineral-Filler Content - Calcination Methods*. Geneva, CH: International Organization for Standardization, 1996.
[27] SIREG. “Technical Data Sheet: Blocking System Carbo. TDS-518.” Arcore, IT, 2019.
[28] PAUL. *Prestressed Concrete Technology: Anchor Grips*. Dürmentingen, DE: Paul International Organization for Standardization, 2009.
[29] SIREG. “Technical Data Sheet: Glasspree® E46 Round Bars and Stirrups. TDS-366.” Arcore, IT, 2019.
[30] CEN. *Eurocode: Basics of Structural Design. EN 1990:2002*. Brussels, BE: European Committee for Standardization, 2002.
[31] Cadenazzi, Thomas, Giovanni Dotelli, Marco Rossini, Steven Nolan, and Antonio Nanni. “Cost and Environmental Analyses of Reinforcement Alternatives for a Concrete Bridge.” *Structure and Infrastructure Engineering*, 2019, 16.
[32] Cadenazzi, Thomas, Giovanni Dotelli, Marco Rossini, Steven Nolan, and Antonio Nanni. “Life-Cycle Cost and Life-Cycle Assessment Analysis at the Design Stage of a Fiber-Reinforced Polymer-Reinforced Concrete Bridge in Florida.” *Advances in Civil Engineering Materials* 8, no. 2 (2019).
[33] Rossini, Marco, Antonio Nanni, Fabio Matta, Steven Nolan, William Potter, and Derek Hess. “Overview of AASHTO Design Specifications for GFRP-RC Bridges 2nd Edition: Toledo Bridge as Case Study.” In *IABSE Symposium: Towards a Resilient Built Environment, Risk and Asset Management - Report*, 1214–21. Guimarães, PT: International Association for Bridge and Structural Engineering, 2019.
[34] R. Haghani and J. Yang, "Application of FRP Materials for Construction of Culvert Road Bridges Manufacturing and life-cycle cost analysis," Chalmers University of Technology, Göteborg (SW), 2016.

Table 1 – List of all specimen tested. (*) indicates runout specimen.

SPECIMEN ID	f_{fu}	$f_{f,pi}$	$f_{f,ps}$	$t_{failure}$	f_{12h} / f_i	$t_{preload}$	τ_{fu}	δ_F
	MPa	MPa	MPa	hours	/	minutes	MPa	mm
STR #1.50-T	851	-	-	-	-	-	-	-
STR #1.75-T	867	-	-	-	-	-	-	-
STR #1.25-P1	-	533	-	-	-	-	-	-
STR #1.25-P2	-	534	-	-	-	-	-	-
STR #1.25-P3	-	519	-	-	-	-	-	-
STR #1.50-P1	-	531	-	-	-	-	-	-
STR #1.50-P2	-	486	-	-	-	-	-	-
STR #1.75-P	-	555	-	-	-	-	-	-
STR #4.50-P	-	510	-	-	-	-	-	-
STR #1.50-CR	-	-	418	3.18	-	-	-	-
STR #1.75-CR	-	-	452	0.13	-	-	-	-
STR #1.25-C	-	-	348	24.1*	-	-	-	-
STR #1.50-C	-	-	349	62.1*	-	-	-	-
STR #1.75-C	-	-	348	39.7*	-	-	-	-
STR #4.50-C	-	-	348	24.0*	-	-	-	-
STR #1.25-R	-	-	-	-	0.81	-	-	-
STR #1.50-R	-	-	-	-	0.83	-	-	-
STR #1.75-R	-	-	-	-	0.79	-	-	-
STR #4.50-R	-	-	-	-	0.77	-	-	-
STR #1.25-RP(1)	-	-	-	-	0.81	1	-	-
STR #4.50-RP(5)	-	-	-	-	0.82	5	-	-
STR #1.75-RP(10)	-	-	-	-	0.88	10	-	-
STR #1.50-RP(15)	-	-	-	-	0.91	15	-	-
STR #1.50-RR	-	-	-	-	0.95	-	-	-
STR #1.75-RR	-	-	-	-	0.97	-	-	-
STR #1.25-S1	-	-	-	-	-	-	156	-
STR #1.25-S1	-	-	-	-	-	-	170	-
STR #1.50-F	-	-	-	-	-	-	-	41

Table 2 – Material properties of constituents and TP composites plus target properties for TP composites.

Property		Constituents		Thermoplastic GFRP			
		Fiber	Resin	Wire	Strand	Bar	Target
f_{fu}	MPa	3450	65.5	891	881	948	844*
E_f	GPa	80.5	3.2	-	45.6	48.0	44.8*
ε_{fu}	/	0.04	0.05	-	0.02	0.02	0.02*
τ_{fu}	MPa	-	-	179	-	-	131*
η_{fu}	MPa	-	-	14.2	-	-	22.6+
χ_{fu}	mm^{-1}	-	-	0.005	-	-	0.003x

* ASTM D7957 requirement for acceptance.

+ Performance of an equivalent VE-GFRP 6-mm bar.

x Required for coilability around a standard 610-mm coil.

Table 3 – Summary of mechanical properties of five alternative GFRP material systems.

Material	a_f	f_{fu}	E_f	ε_{fu}	τ_{fu}	η_{fu}	χ_{fu}	D_R
	mm^2	MPa	GPa	%	MPa	MPa	mm^{-1}	mm
STR/TP	141.1	881	45.6	1.9%	0	14.2	0.0054	393
M13/TP	116.0	948	48.0	2.0%	-	-	0.0010	2,000*
STR/VE	127.8	859	44.5	1.9%	163	22.6	0.0013	1,507
M13/VE	129.7	910	45.5	2.0%	193	33.8	0.0010	2,000*
M16/VE	200.9	763	46.3	1.6%	188	30.2	-	-

* Typical spool diameter currently used for shipping of M13 GFRP bars.

Table 4 – Summary of pull properties of alternative GFRP material systems coupled with various anchors.

Material system	$f_{f,pi}$	$f_{f,pi}^*$	*COV*	*Slippage*
	MPa	MPa	/	mm
STR/TP/ST	126	-	-	13.1
STR/TP/EP	559	-	-	17.7
STR/VE/ST	524	464	3.8%	11.1
M16/VE/ST	586	502	4.8%	8.8
M13/VE/ST	625	564	3.2%	5.9
M13/VE/NY	611	460	8.2%	9.9

Table 5 – Summary of pseudo-creep properties of VE-GFRP material systems coupled with ST anchors.

Material system	$f_{f,js}$	d_{12h}/d_i	$\Delta d_{12h}/d_i$
	MPa	/	/
STR/VE/ST-C	348	1.11	0.11
M16/VE/ST-C	288	1.05	0.05
M13/VE/ST-C	309	1.04	0.04

Table 6 – Summary of pseudo-relaxation properties of VE-GFRP material systems with ST and NY anchors.

Material system and test procedure	f_i	f_{12h}	f_{12h}/f_i	$\Delta f_{12h}/f_i$	$t_{preload}$	N_{reload}	t_{reload}	Seating losses
	MPa	MPa	/	/	min	/	min	
ST/VE/STR-R	348	279	0.80	0.20	-	-	-	10.2%
M16/VE/ST-R	299	254	0.85	0.15	-	-	-	7.7%
M13/VE/NY-R	309	281	0.91	0.09	-	-	-	4.7%
STR/VE/ST-RP(1)	348	282	0.81	0.19	1	-	-	9.7%
STR/VE/ST-RP(5)	348	287	0.82	0.18	5	-	-	9.0%
STR/VE/ST-RP(10)	348	307	0.88	0.12	10	-	-	6.0%
STR/VE/ST-RP(15)	348	315	0.91	0.09	15	-	-	4.9%
M16/VE/ST-RE(1x20)	311	278	0.89	0.11	-	1	20	5.5%
M16/VE/ST-RE(1x60)	316	287	0.91	0.09	-	1	60	4.7%
STR/VE/ST-RE(1x720)	348	334	0.96	0.04	-	1	720	2.0%
M16/VE/ST-RE(2x20)	303	269	0.89	0.11	-	2	20	5.8%

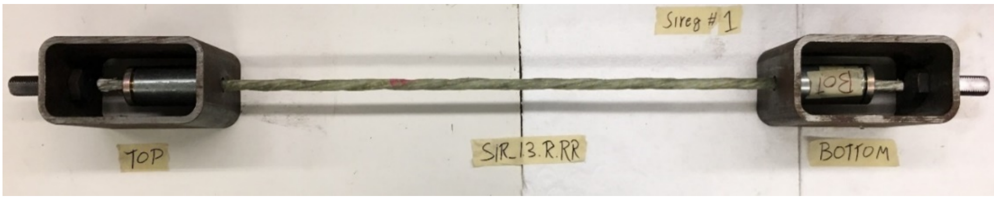

Figure 3 – GFRP strand ready for pull test.

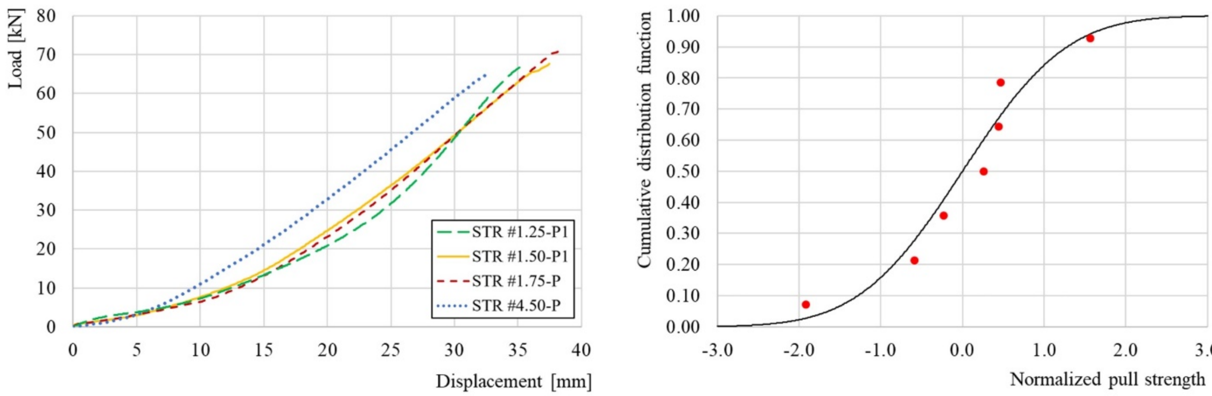

Figure 4 – Pull test results for representative specimens (a), and statistical distribution of pull test results.

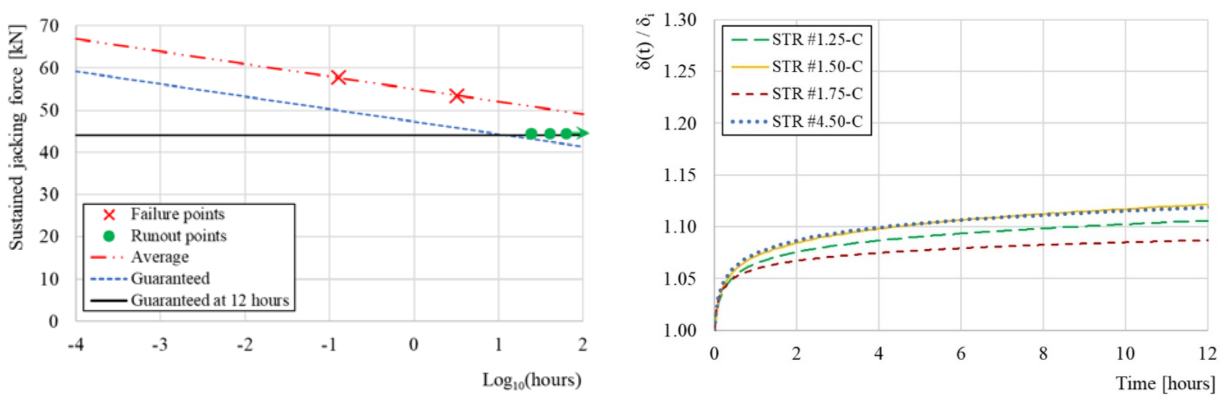

Figure 5 – Average and guaranteed pseudo-creep-rupture curves for the GFRP strand-anchoring system (a) and total pseudo-creep displacement under sustained load.

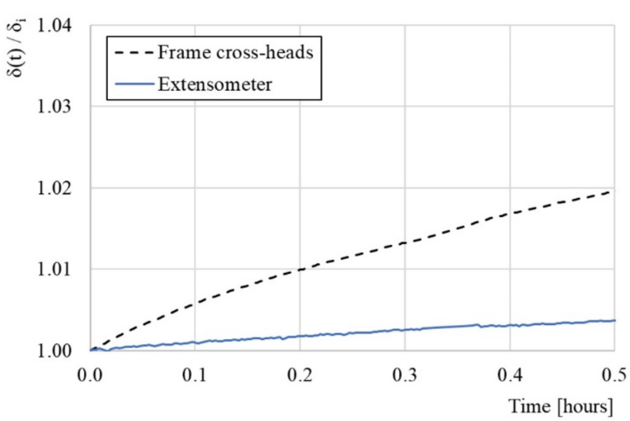

Figure 6 – Total displacement (frame cross-heads) and creep contribution (extensometer) under sustained load.

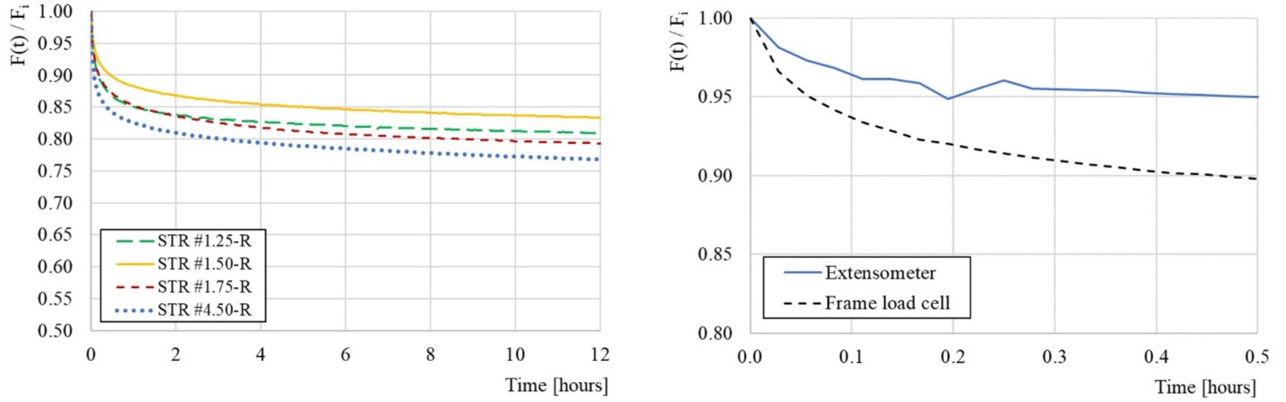

Figure 7 – Retained load under sustained displacement (a) and total retained load (load cell) compared to slipping contribution (extensometer) under sustained displacement.

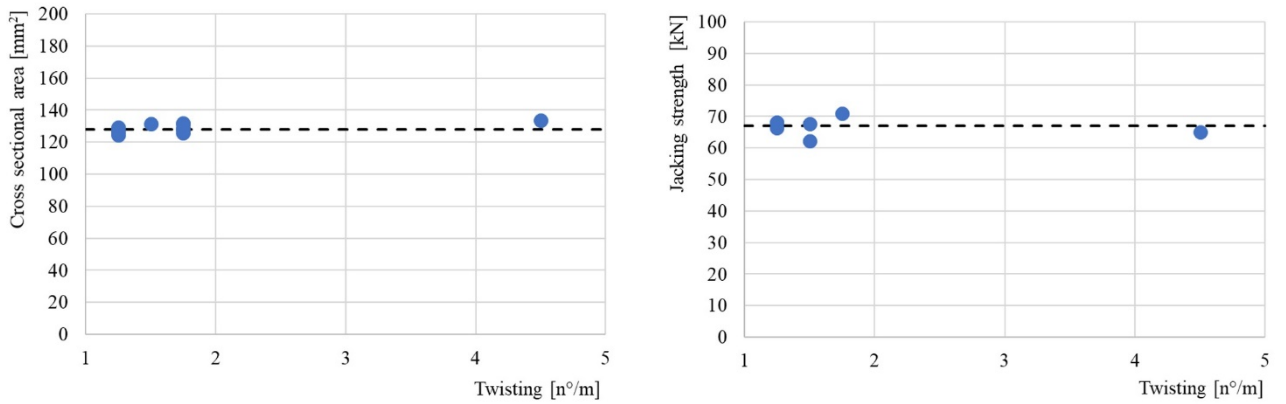

Figure 8 – Cross-sectional area at varying twist per meter (a) and pull strength at varying twist per meter (b).

Figure 9 – Experimental setup for flexural test.

Figure 10 – TP-GFRP material systems developed: 5-mm wire (left), 15.2-mm twisted strand (center), 12-mm reinforcing bar (bottom).

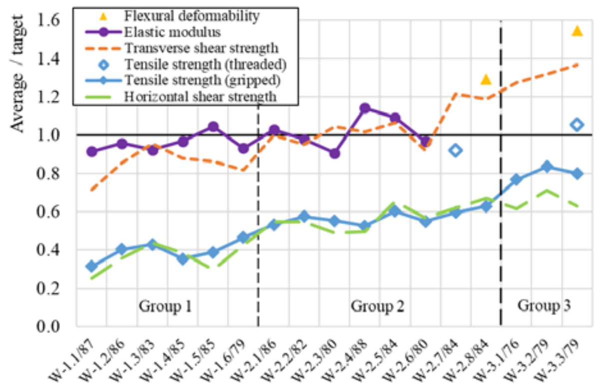

Figure 11 – Performance of different batches of TP-GFRP wire as a ratio to their target.

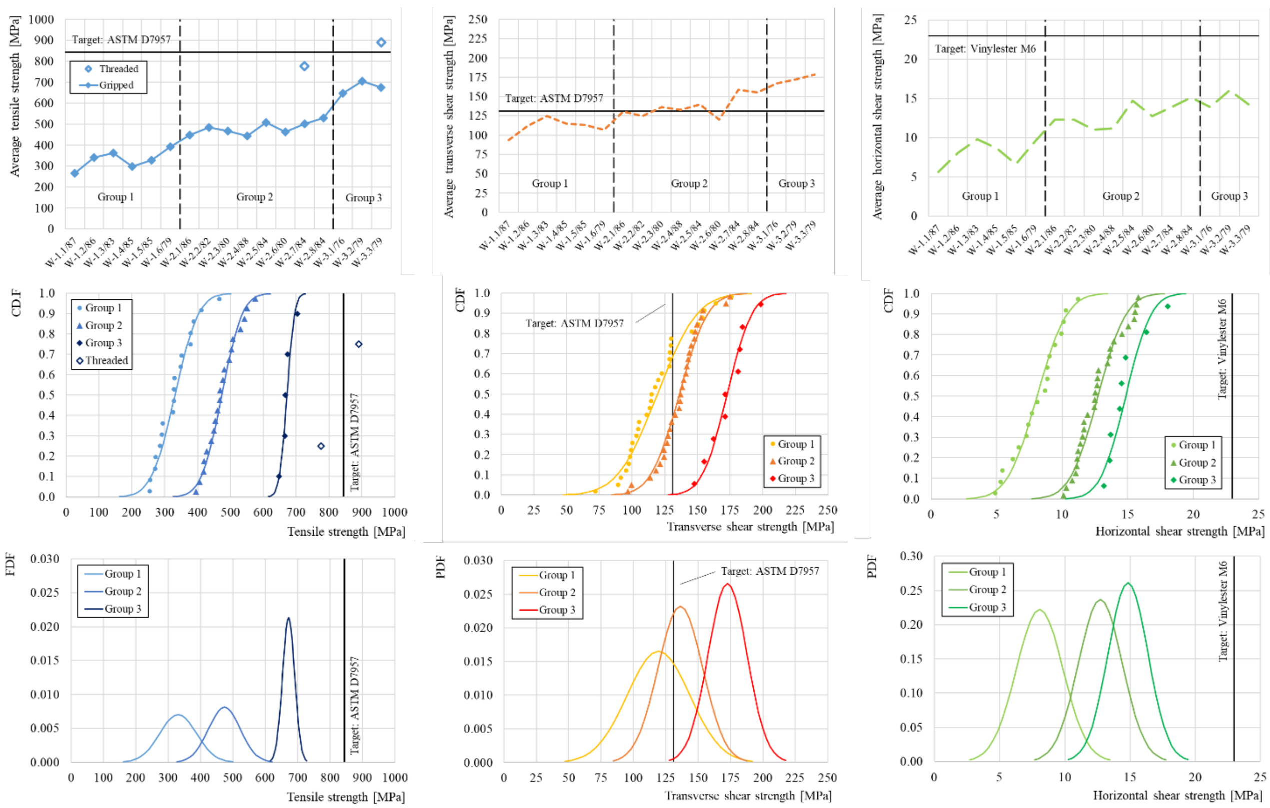

Figure 12 – Left column: evolution of tensile strength of TP-GFRP wires (top) and its statistical distributions as CDF (center) and PDF (bottom). Center column: evolution of transverse shear strength of TP-GFRP wires (top) and its statistical distributions as CDF (center) and PDF (bottom). Right column: evolution of interlaminar shear strength of TP-GFRP wires (top) and its statistical distributions as CDF (center) and PDF (bottom).

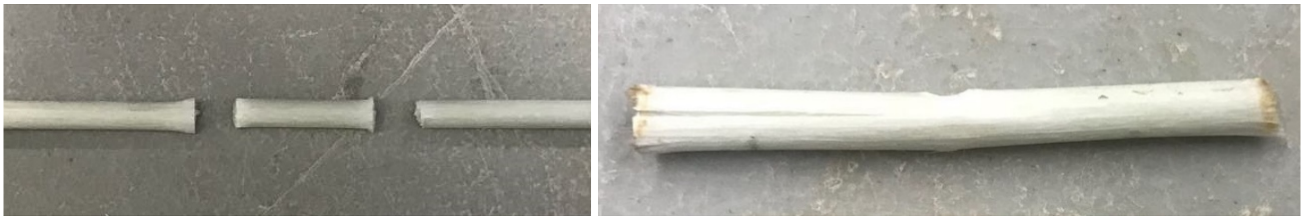

Figure 13 – Typical failure mode for transverse shear tests (left) and interlaminar shear tests (right).

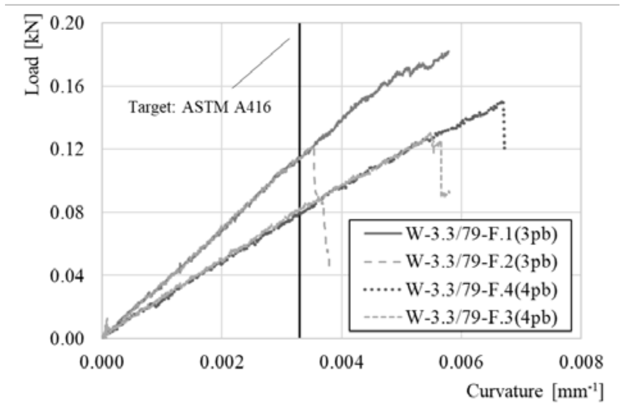

Figure 14 – Load-curvature diagrams of flexural tests performed on production batch W-3.3/79.

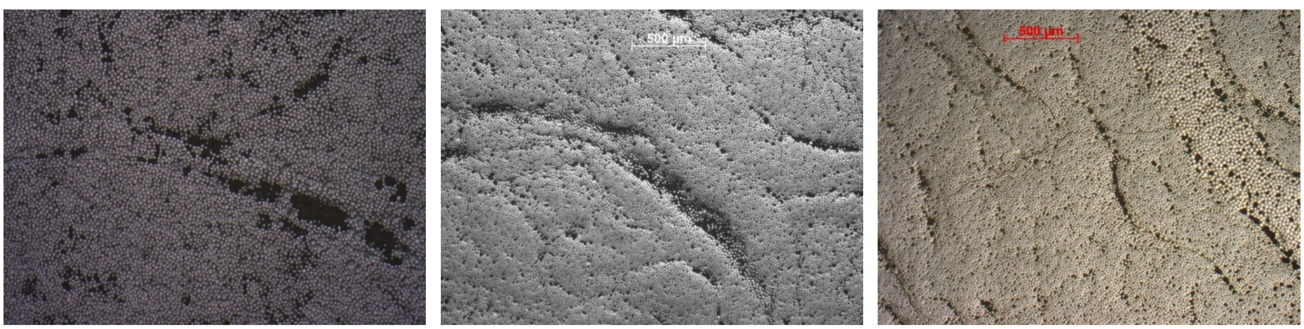

Figure 15 – Microstructure of samples extracted from Group 1 (a), Group 2 (b), and Group 3 (c). All figures use the same scale

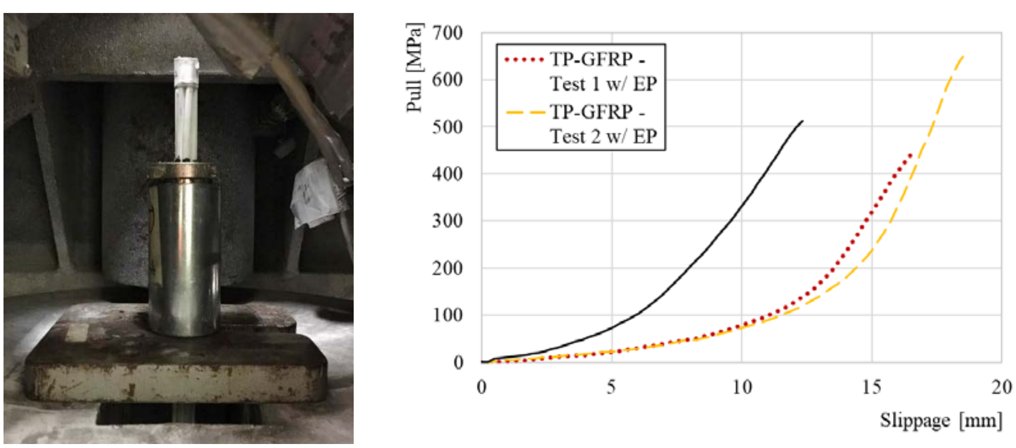

Figure 16 – Details of a TP-GFRP strand coupled with a traditional pre-tensioning steel anchor and ready for testing (left), and stress-slippage diagrams of the TP-GFRP strands tested with EP coating compared to a typical VE-GFRP strand (right).

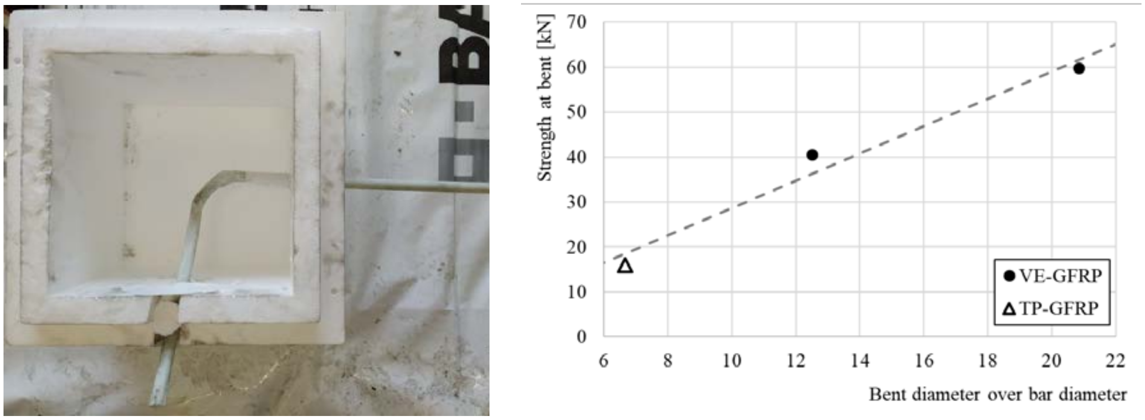

Figure 17 – Setup for the bent strength test (left) and bent strength plotted against the ratio of bend diameters over bar diameter (right).

Figure 18 – Traditional Steel (ST) anchors [top], detail of Epoxy (EP) coating after testing [center], alternative anchor with Nylon (NY) wedges [bottom].

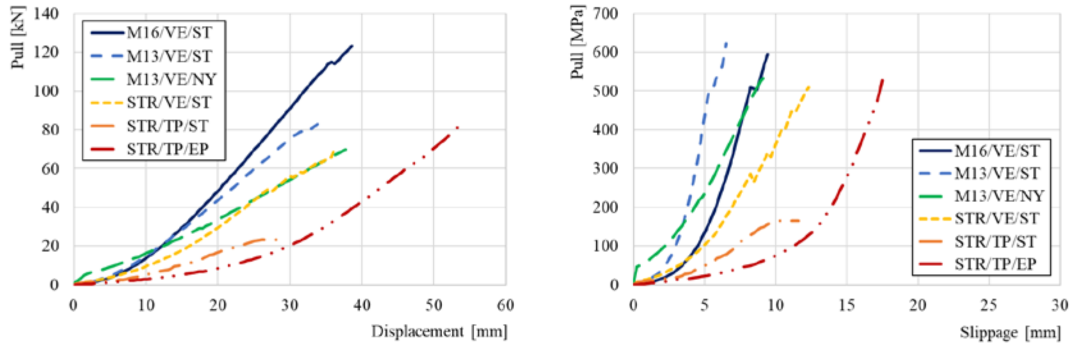

Figure 19 – Comparison of the pull performance of various materials and anchoring systems

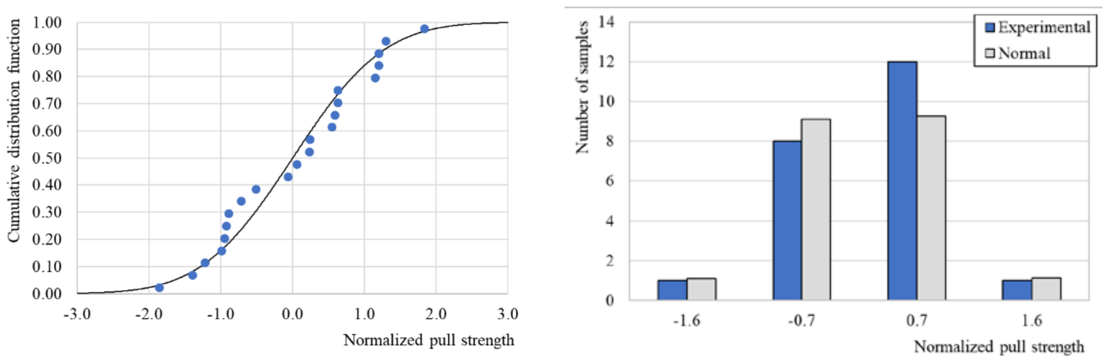

Figure 20 – Statistical distribution of pull strength results for VE-GFRP material systems.

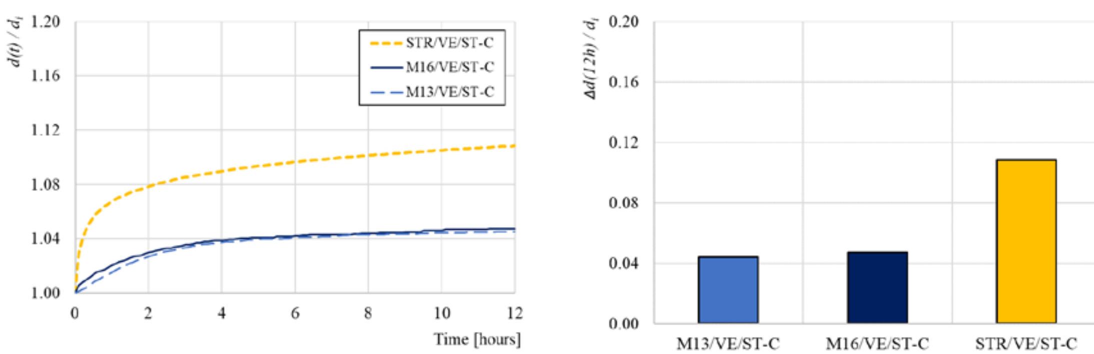

Figure 21 – Comparison of the pseudo-creep performance of VE-GFRP reinforcement with ST anchors.

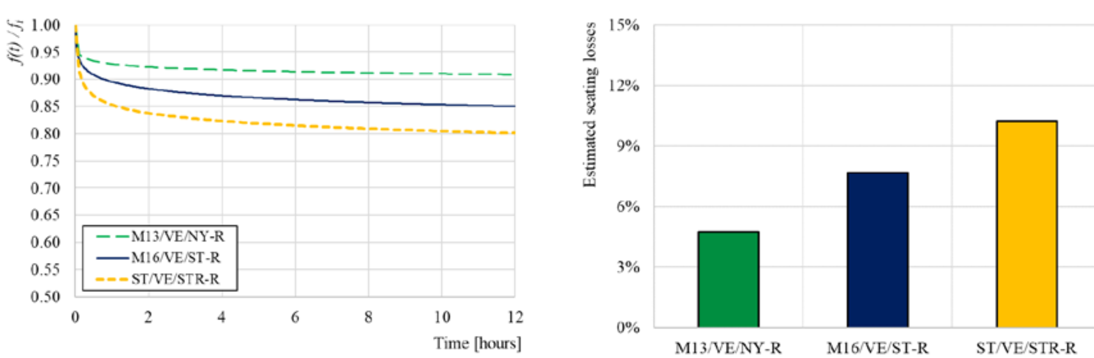

Figure 22 – Comparison of the pseudo-relaxation performance (left) and seating losses (right) of VE-GFRP reinforcement with NY and ST anchors.

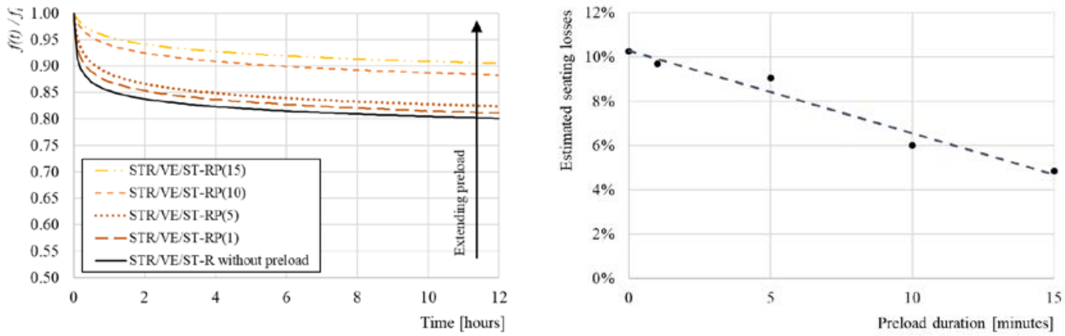

Figure 23 – Pseudo-relaxation performance of VE-GFRP reinforcement with preload.

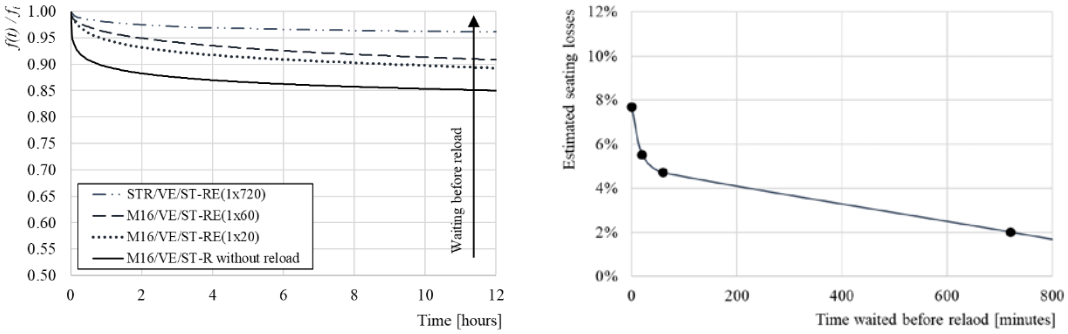

Figure 24 – Pseudo relaxation performance of VE-GFRP reinforcement with reload.

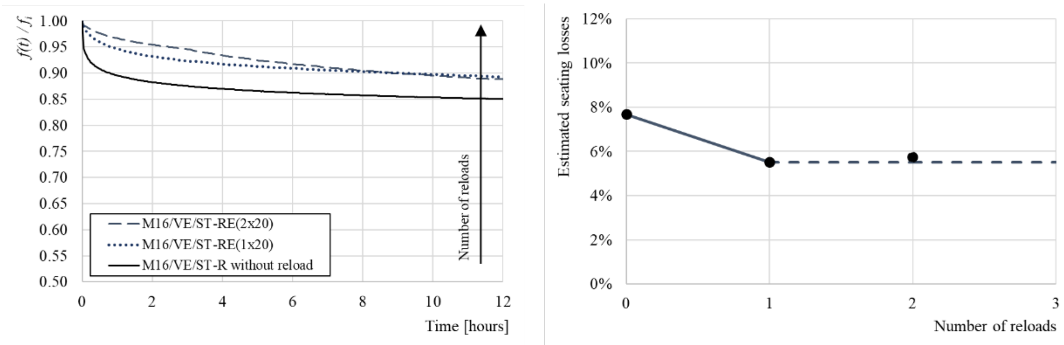

Figure 25- Pseudo relaxation performance of VE-GFRP reinforcement with multiple preloads.

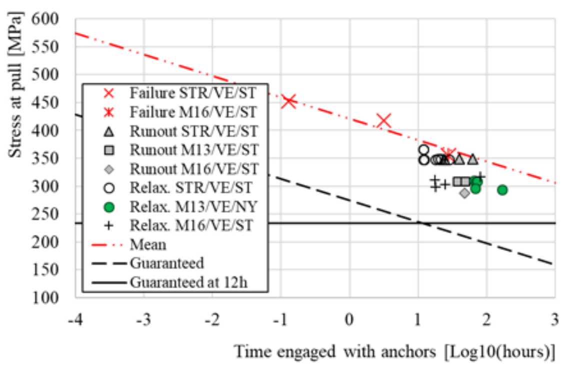

Figure 26 – Pseudo-creep-rupture diagram of VE-GFRP with ST anchors and runout points for NY anchors.

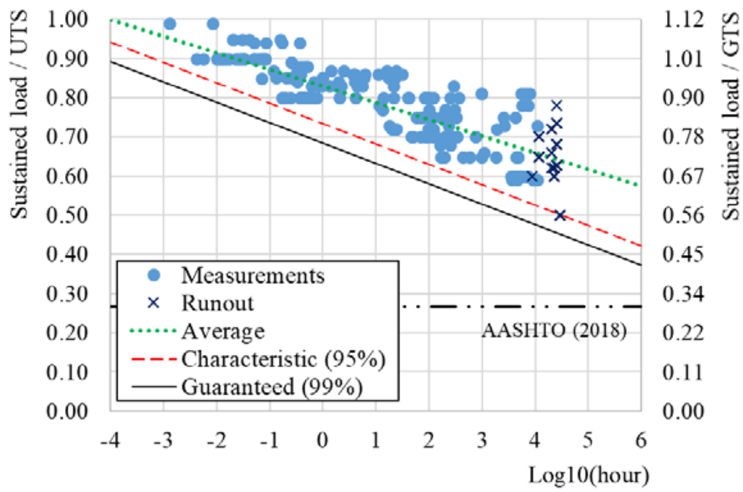

Figure 27 – Evaluation of the creep-rupture strength of VE-GFRP reinforcement.

Figure 28 – Construction of the structural members for testing at the University of Houston.

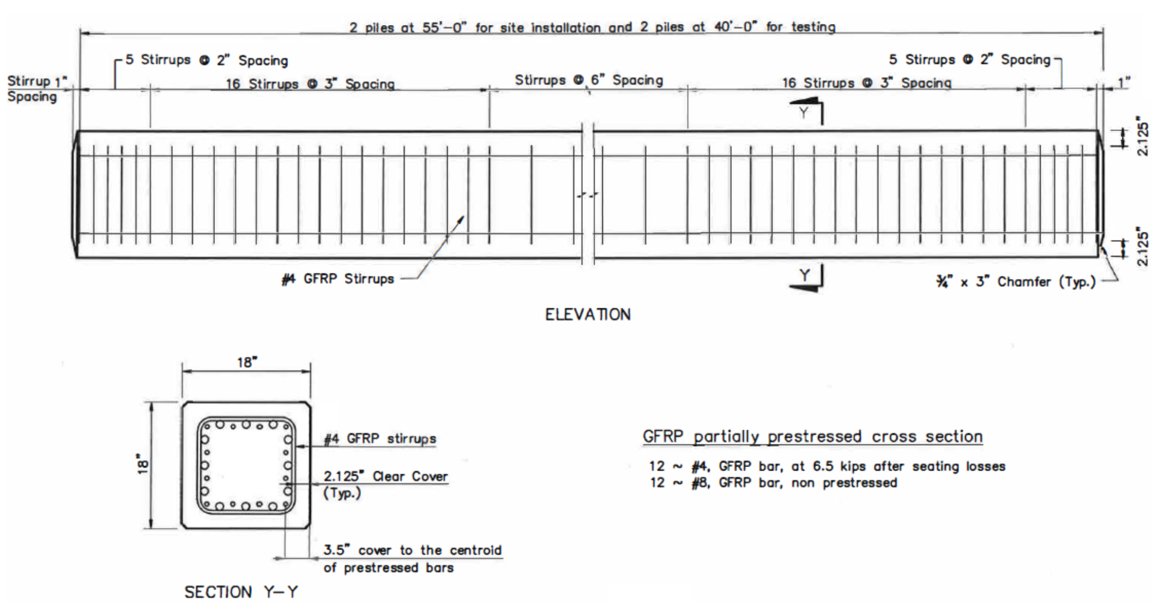

Figure 29 – Design of the demonstrative piles under construction at the 23rd Avenue Bridge over Ibis Waterway.

APPENDIX 1: RESEARCH RESULTS

Sidebar information

Program Steering Committee: NCHRP-IDEA Program Committee
Title: MILDGLASS: GFRP Strand for Resilient Mild Pre-Stressed Concrete
Project Number: NCHRP-IDEA/207
Start Date: April 25th, 2018
Completion Date: April 24th, 2020
Investigators: Antonio Nanni, Marco Rossini
Institution: University of Miami
Email: nanni@miami.edu
Phone: 305 284 3461

TITLE: MILDGLASS: GFRP Strand for Resilient Mild Pre-Stressed Concrete

SUBHEAD: This project develops a resilient and cost-effective GFRP prestressing tendon

WHAT WAS THE NEED?

Corrosion of steel reinforcement is the primary cause of durability problems in aged Reinforced- and Prestressed-Concrete (RC and PC) structures. The legacy of the extensive transportation infrastructure development and expansion, in combination with aggressive environments, represents a critical Maintenance, Rehabilitation and Replacement (MRR) liability at the national scale. The construction industry has only partially answered the rising demand for corrosion-resistant technologies, offering expensive, complex and sometimes ineffective solutions.

WHAT WAS OUR GOAL?

This project developed corrosion-resistant tendons for PC application that, in addition to durability and mechanical performance, exhibits favorable constructability and cost characteristics.

WHAT DID WE DO?

The focus of this project is Glass Fiber Reinforced Polymer (GFRP) that retains immunity to corrosion and maintains a material cost comparable to traditional carbon steel reinforcement while showing higher strain at failure and significantly lower modulus of elasticity with respect to other non-corrosive reinforcing solutions such as High Strength Stainless Steel (HSSS) and Carbon FRP (CFRP). The low modulus is an advantageous feature in PC construction during fabrication (larger and more controllable displacement at prestressing) and design (lower elastic shortening).

WHAT WAS THE OUTCOME?

This project developed various GFRP material solutions that are coilable and may be used in prestressing applications. These include: (a) a 15.2-mm 7-wire GFRP strand prototype developed using Electrical/Chemical Resistant (ECR) glass fibers and thermosetting Vinyl Ester resin (VE) shown at the top left of Figure 1; (b) a 15.2-mm -wire GFRP strand prototype developed using ECR glass fibers and ThermoPlastic (TP) acrylic resin shown at the top right of Figure 1; (c) a 12.7-mm (M13) coilable GFRP bar made with ECR glass fibers and VE resin shown at the bottom left of Figure 1; and, (d) a 12-mm bendable GFRP bar made with ECR glass fibers and TP resin shown at the bottom right of Figure 1. Two different anchoring systems were evaluated: traditional Steel (ST) prestressing anchors, and an equivalent anchoring system that uses polymeric Nylon (NY) wedges that have a softer interaction with the surface of the reinforcement. Results showed GFRP tendons compatibility with traditional pulling procedures. Two demonstrative piles partially-prestressed using coilable M13/VE-GFRP straight bars and NY anchors have been constructed for installation at the FDOT-managed 23rd Avenue Bridge over Ibis Waterway in Broward County, FL (Figure 2).

WHAT IS THE BENEFIT?

GFRP tendons provide a cost-effective non-corrosive alternative to traditional steel strands in applications that require relatively low levels of prestress and are located in aggressive and corrosive environments. GFRP tendons can be effectively coupled with simple anchoring systems guaranteeing adequate pull strengths and low seating losses. The ability to couple GFRP tendons with simple anchors will minimize impact on traditional precasting operations. The use of TP resin is an innovative solution that eases manufacturing of complex shapes by allowing thermoforming, post-heating, and staged manufacturing. It may have a disruptive impact on the composite reinforcement industry providing effective and efficient solutions to foster the durability of transportation infrastructures. The innovation associated with the use of TP resin in GFRP reinforcement was recognized by the 2019 JEC Innovation Award in Construction and Infrastructures presented to a joint partnership of Arkema, SIREG NCHRP, and the University of Miami for the work developed within the MILDGLASS project. JEC Group is the world's leading company dedicated to the development of the composite industry.

LEARN MORE

To learn more, find the final project report at: http://www.trb.org/Publications/PubsIDEAHighwayFinalReports.aspx; follow the project newsfeed at: https://www.researchgate.net/project/MILDGLASS-GFRP-Strand-for-Resilient-Mild-Prestressed-Concrete; contact Dr. Antonio Nanni at nanni@miami.edu or Dr. Marco Rossini at mxr1465@miami.edu.

Figure 1 – GFRP/VE 15.2-mm strand compared to a CFRP commercial solution (top left), 15.2-mm GFRP/TP strand (top right), GFRP/VE 12-mm coilable bar (bottom left), GFRP/TP 12-mm coilable bar (bottom right).

Figure 2 – Construction of two partially-prestressed piles serving as demonstrator for the MILDGLASS concept.

APPENDIX 2: LIFE CYCLE COST ANALYSIS

Note from the authors

This document is prepared as Appendix 2 of the NCHRP-IDEA/207: MILDGLASS Final Report to answer the demand by the Florida Department of Transportation (FDOT) for a simplified procedure to perform Life Cycle Cost (LCC) to be used as a support for decision-making in future projects.

TITLE: Simplified Approach to Comparative Life Cycle Cost Analysis of Alternative Reinforcement Solutions

AUTHORS: Marco Rossini (mxr1465@miami.edu), Antonio Nanni (nanni@miami.edu)

INTRODUCTION

This document presents a simplified approach to perform a comparative Life Cycle Cost (LCC) analysis of different reinforcement alternatives for 457-mm square piles designed according to:

A. FDOT Index No. 20618 for 457-mm square piles prestressed with 12 ~ 15.2-mm High Strength Carbon Steel (HSCS) strands and transversally reinforced with Mild Carbon Steel (MCS) spiral ties of 5.3-mm diameter at a pitch ranging from 75 mm to 150 mm.
B. Option B is the same as Option A but using High Strength Epoxy-coated Steel (HSES) and Mild Epoxy-coated Steel (MES). Epoxy-coated steel cannot be used in FDOT projects and is here considered only for comparison.
C. FDOT Index No. 22618 (sheet 2) for 457-mm square piles prestressed with 16 ~ 12.7-mm High Strength Stainless Steel (HSSS) strands and transversally reinforced with Mild Stainless Steel (MSS) spiral ties of 5.7-mm diameter at a pitch ranging from 75 mm to 150 mm.
D. FDOT Index No. 22618 (sheet 1) for 457-mm square piles prestressed with 12 ~ 15.2-mm Carbon Fiber Reinforced Polymer (CFRP) strands and transversally reinforced with CFRP spiral ties of 5-mm diameter at a pitch ranging from 75 mm to 150 mm.
E. Equivalent design proposed by the University of Miami for 457-mm square piles partially prestressed with 12 ~ 12.7-mm Glass Fiber Reinforced Polymer (GFRP) pre-tensioned bars, 12 ~ 25.4-mm GFRP (GFRP) non pre-tensioned bars, and transversally reinforced with GFRP ties of 12.7-mm diameter at a spacing ranging from 75 mm to 150 mm.
F. Option F is the same as Option E but uses a different concrete mix based on a ternary binder of Calcium SulfoAluminate (CSA) clinker, Portland cement, and anhydrite instead of Ordinary Portland Cement (OPC) alone. Concrete mixed with CSA-based ternary binders have appealing features including fast setting and high strength development. These concrete mixes may improve the durability of GFRP bars thanks to their relatively low pH.

INITIAL COST

Costs for material, equipment, transportation, installation, and personnel, are taken and adapted from Cadenazzi et al. [31, 32] and Rossini et al. [33]. Construction time and crews are taken as reported by Cadenazzi et al. [31, 32] for the construction of similar elements. The cost of a CSA-based concrete mix is estimated at 1.2 times the cost of an equivalent FDOT Class V special mix. Material costs for longitudinal and transverse reinforcement are summarized as follows:

- The material cost of HSCS 15.2-mm strands can be estimated at 3.3 $/m; the material cost of HSES 15.2-mm strands can be estimated at 3.9 $/m; the material cost of 12.7-mm HSSS strands can be estimated at 13.1 $/m; the material cost of 15.2-mm CFRP strands can be estimated at 12.5 $/m; the material cost of 12.7-mm GFRP bars can be estimated at 1.9 $/m; the material cost of 25.4-mm GFRP bars can be estimated at 6.3 $/m.
- The material cost of MCS 5.3-mm spiral ties can be estimated at 0.24 $/m; the material cost of MES 5.3-mm spiral ties can be estimated at 0.28 $/m; the material cost of MSS 5.7-mm spiral ties can be estimated at 1.1 $/m; the material cost of 5-mm CFRP spiral ties can be estimated at 1.8 $/m; the material cost of 12.7-mm GFRP ties can be estimated at 2.9 $/m.

The initial cost of HSCS-prestressed piles after installation can be computed as 330 \$/m. The initial cost of HSES-prestressed piles after installation can be computed as 339 \$/m (+2.7%). The initial cost of HSSS-prestressed piles after installation can be computed as 532 \$/m (+61%). The initial cost of CFRP-prestressed piles after installation can be computed as 538 \$/m (+63%). The initial cost after installation of GFRP-partially-prestressed piles can be computed as 412 \$/m (+25%). The initial cost after installation of GFRP-partially-prestressed piles with CSA-based concrete can be computed as 416 \$/m (+26%). Initial costs for the six alternatives are shown in Figure 1a.

LIFE CYCLE COST

The HSCS and HSES alternatives are designed for a service life (L) of 75 years including maintenance operations. The HSSS, CFRP, and the two GFRP alternatives are designed for a service life of 100 years with only minimal concrete patching. Maintenance models and costs are taken as reported by Cadenazzi et al. [31, 32] for similar structures. Maintenance costs for the HSCS alternative can be computed as 122% of the initial cost; maintenance costs for the HSES alternative can be computed as 72% of the initial cost; maintenance costs for the HSSS, CFRP, and for the two GFRP alternatives can be computed as 6.6% of the initial cost.

The maintenance costs are distributed over the respective life span of each structure and discounted to present value assuming a discount rate (r) equal to 1% as suggested by Cadenazzi et al. [31, 32]. This allows to compute the Net Present Cost (NPC) of each alternative including initial cost and discounted maintenance operations. Building on the work of Haghani & Yang [34] as proposed by Rossini et al. [33], the NPC can be normalized over a uniform service life to compute the Equivalent Cost (EC) that allows for direct comparison between design alternatives characterized by different service lives. The EC at 100 years for each design alternative can be computed using Eq. 1.

$$EC_i = NPC_i \, \frac{1-(1+r)^{-100}}{1-(1+r)^{-L_i}} \tag{1}$$

The 100-year EC for the HSCS-prestressed alternative can be computed as 727 \$/m; the 100-year EC for the HSES-prestressed alternative can be computed as 605 \$/m (-17%); the 100-year EC for the HSSS-prestressed alternative can be computed as 557 \$/m (-23%); the 100-year EC for the CFRP-prestressed alternative can be computed as 563 \$/m (-23%); the 100-year EC for the GFRP-partially-prestressed alternative can be computed as 430 \$/m (-41%); the 100-year EC for the GFRP-partially-prestressed alternative with CSA-based concrete can be computed as 435 \$/m (-40%). 100-year ECs for the six alternatives are shown in Figure 1b.

CONCLUSIONS

The simplified analysis performed shows how the proposed GFRP-partially-prestressed option is the most convenient in terms of Life Cycle Cost (LCC) with savings at 40-41% with respect to HSCS and an initial cost only 25-26% higher. The proposed method is a viable simplified approach to life cycle costing and can be used for rapid estimation to support decision-making. The higher cost of concrete mixed with CSA-based ternary binders has only a minimal impact on the overall cost of structural elements. These types of concrete mixes may have positive implications on the durability of GFRP reinforcement and on the mechanical performance and speed of production of structural members. The production of CSA-based ternary binders features a reduced carbon footprint with respect to OPC. Furthermore, the lower pH of CSA-based mixes may enhance the environmental compatibility of concrete structures and their integration within existing ecosystems.

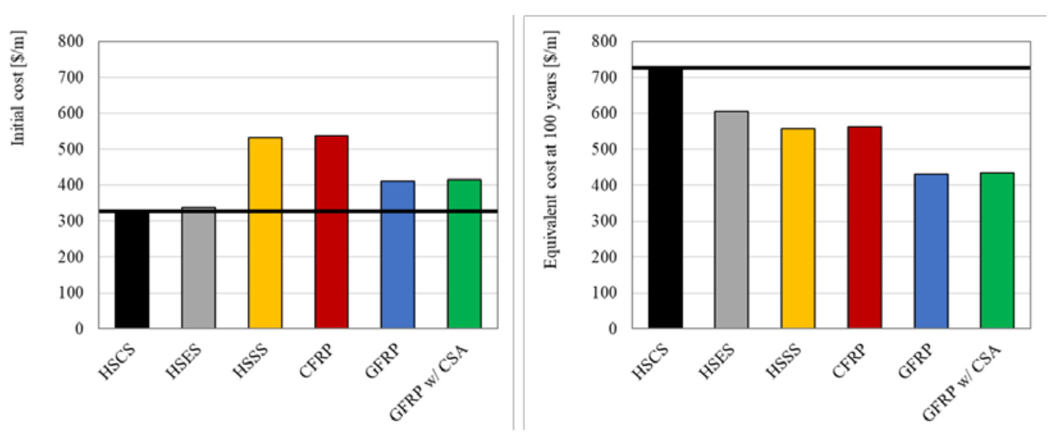

Figure 1 – Initial cost (left) and 100-year equivalent cost (right) of six design alternatives for 457-mm square piles.

APPENDIX 3: DISSEMINATION AND IMPLEMENTATION

Note from the authors

This Appendix of the NCHRP-IDEA/207: MILDGLASS Final Report details the efforts undertaken to ensure dissemination of the findings of this study and promote further implementation and exploitation of GFRP prestressing in transportation infrastructures. Dissemination, communication, and implementation efforts are divided by target stakeholder sector and audience. The text uses hyperlinks and should be consulted in its digital form for an optimal fruition.

NCHRP-IDEA AND FEDERAL TRANSPORTATION AGENCIES

MILDGLASS was selected to be included in the 2020 NCHRP-IDEA Report to the AASHTO Research and Innovation Committee as a project with a high potential for implementation and commercialization. The concept and outcomes of MILDGLASS were presented at the 2020 TRB Annual Meeting, and at the 2018 International Highway Engineering Exchange Program Conference. MILDGLASS appears in multiple NCHRP-IDEA annual reports.

The University of Miami (UM) contributed to the works of the taskforce responsible for drafting the second edition of the AASHTO Bridge Design Guide Specifications for GFRP-Reinforced Concrete. A similar regulatory process is desirable once GFRP prestressing achieves full commercial development.

FLORIDA DEPARTMENT OF TRANSPORTATION

MILDGLASS interacts synergistically with a transversal initiative initiated by the Florida Department of Transportation (FDOT) to promote the use of FRP reinforcement in the State of Florida. The University of Miami (UM) is integral part of several components of this initiative that includes the organization of seminars and workshops, the deployment of FRP reinforcement in bridges and coastal structures, the delivery of courses aimed at educating bridge engineers from Florida on how to design structures using GFRP reinforcement, and the development of codes and standards.

FDOT is a key stakeholder in the MILDGLASS project with the 23rd Avenue Bridge over Ibis Waterway in Broward County (FL) serving as the first full-scale demonstrator of the MILDGLASS concept. The UM Structures and Materials Lab (SML) is an FDOT-authorized laboratory that has tested for acceptance the coilable M13/VE-GFRP bars used in the MILDGLASS demonstration and is proceeding to full certification per FDOT specifications and ASTM standards. This step will make the material system deployable in any transportation project in Florida. The successful examples brought forward by FDOT are expected to promote the adoption of this technology among other states.

COMPOSITE AND CONSTRUCTION INDUSTRY

The innovation associated with the use of TP resin in GFRP reinforcement was recognized by the 2019 JEC Innovation Award in Construction and Infrastructures presented to a joint partnership of Arkema, NCHRP, SIREG, and UM for the work developed within the MILDGLASS project. This recognition highlights the interest expressed by the composite industry in this technology, its relevant implications on the GFRP reinforcement supply chain, and its ability to better serve the needs of the transportation community.

Several industrial partners were involved in the MILDGLASS project and maintain their commitment to leverage the diffusion of the technology. FRP manufacturers such as Owens Corning and SIREG have certified or are certifying their materials for use in transportation projects nationwide. Furthermore, industry partners are actively promoting the use of GFRP among transportation officials and bridge engineers. Gate Precast has been and is actively involved in several projects involving FRP prestressing including constructing the GFRP partially prestressed piles serving as MILDGLASS demonstrator. Arkema is proactively developing and improving thermoplastic resins for use in GFRP reinforcement. Buzzi Unicem is investigating synergies between innovative cements and concrete mixes and composite reinforcement. These virtuous examples are contributing to assemble a solid knowledge and confidence base among stakeholders.

SCIENTIFIC COMMUNITY

MILDGLASS features synergies with the HuRRI Composites research effort that aims to improve the resilience of coastal communities and infrastructures. Furthermore, the results gathered by MILDGLASS may prove beneficial for NCHRP-IDEA/213: SEAHIVE. The dissemination of the results of the MILDGLASS project took advantages of various channels including a project newsfeed and several publications. A complete list is provided in conclusion of this appendix.

Journal Papers and Special Publications

Rossini, M., Spadea, S., & Nanni, A. (2019). Pedestrian Bridge as Clarifying Example of FRP-RC/PC Design. *ACI Special Publication*, *333–6*, 96–118. Link

Rossini, M., Saqan, E., & Nanni, A. (2019). Prediction of the Creep Rupture Strength of GFRP Bars. *Construction and Building Materials*, *227*, 116620(1-11). Link

Rossini, M., & Nanni, A. (2019). Composite Strands for Prestressed Concrete: State-of-the-practice and Experimental Investigation into Mild Prestressing with GFRP. *Construction and Building Materials*, *205*, 486–498. Link

Spadea, S., Rossini, M., & Nanni, A. (2020). Discussion of "Effect of Prestressing Level on the Time-Dependent Behavior of GFRP Prestressed Concrete Beams" by Mohamed Zawam et al. *JCC*, *24*(1), 1–2. Link

Cadenazzi, T., Dotelli, G., Rossini, M., Nolan, S., & Nanni, A. (2019). Cost and Environmental Analyses of Reinforcement Alternatives for a Concrete Bridge. *Structure and Infrastructure Engineering*, 16. Link

Cadenazzi, T., Dotelli, G., Rossini, M., Nolan, S., & Nanni, A. (2019). Life-Cycle Cost and Life-Cycle Assessment Analysis of an FRP-Reinforced Concrete Bridge in Florida. *Advances in Civil Engineering Materials*, *8*(2). Link

Benmokrane, B., Brown, V. L., Mohamed, K., Nanni, A., Rossini, M., & Shield, C. (2019). Creep-Rupture Limit for GFRP Bars Subjected to Sustained Loads. *Journal of Composites for Construction*, *23*(6), 06019001(1-7). Link

Presentations and Conference Proceedings

Rossini, M., Saqan, E., Pulvirenti, G., & Nanni, A. (2019). Creep Rupture Testing of GFRP Bars under Sustained Loading. In *The 14th International Symposium on FRP Reinforcement (FRPRCS-14)*. Belfast, UK. Link

Rossini, M., Nolan, S., Lasa, I., & Nanni, A. (2019). New Directions for RC: Avoiding Time-bombs in our Coastal Structures. In *Bridge Engineering Institute Conference (BEI-2019)* (pp. 421–426). Honolulu (HI). Link

Rossini, M., Jalles, P., Balconi, G., & Nanni, A. (2018). GFRP Strand Prototype: Experimental Investigation and Technology Readiness. In *the 9th International Conference on FRP Composites (CICE 2018)*. Paris, FR. Link

Rossini, M., & Nanni, A. (2019). MILDGLASS: GFRP Strand Prototype Development. In *Concrete Convention and Exposition (ACI Fall 2019)*. Cincinnati (OH): American Concrete Institute. Link

Rossini, M. (2018). Resilient Transportation Infrastructures: The Innovation Bridge. In *International Highway Engineering Exchange Program Conference (IHEEP 2018)* (p. 48). Lincoln, NE. Link

Nolan, S., Rossini, M., & Nanni, A. (2018). Seawall-Bulkheads, SEACON, Sustainability and Resilience. In *the 5th International fib Congress Proceedings (fib 2018)*. Melbourne, AU. Link

Nolan, S., Freeman, C., Kelley, A., & Rossini, M. (2018). Advancing Small Bridges (Florida-down Under). In *the 5th International fib Congress Proceedings (fib 2018)*. Melbourne, AU. Link

Nolan, S., Cadenazzi, T., Rossini, M., Nanni, A., Knight, C., & Lasa, I. (2019). The 200-year Bridge Substructure: Resilience and Sustainability. In *20th Congress of IABSE: The Evolving Metropolis (IABSE 2019 NY)*. Link

Nolan, S. (2018). Florida's Fiber-reinforced Polymer (FRP) Initiatives for Bridges. In *International Symposium on Advanced Composite Structures*. Link

Nolan, S., Rossini, M., & Nanni, A. (2018). Seawall-Bulkheads, SEACON, Sustainability and Resilience. In *the 5th International fib Congress Proceedings (fib 2018)*. Melbourne, AU. Link

Technical Reports and Other Publications

Nanni, A., Belarbi, A., Dawood, M., Gangone, M., Rossini, M., Rhode-Barbarigos, L., Haus, B. & Cigada, A. (2020). *HuRRI-Composites: Resilient Coastal Communities Using Advanced Construction Materials and Systems.* Link

Nanni, A., Rossini, M., Dotelli, G., & Spadea, S. (2019). MILDGLASS: GFRP Strands for Resilient Mild Prestressed Concrete. In *NCHRP-IDEA Annual Progress Report: New IDEAS for Highway Systems*. Washington, DC. Link

Nanni, A., Rossini, M., Dotelli, G., & Spadea, S. (2020). MILDGLASS: GFRP Strand for Resilient Mild Prestressed Concrete. In *NCHRP-IDEA Annual Progress Report: New IDEAS for Highway Systems*. Washington, DC. Link

Nanni, A., Rossini, M., Dotelli, G., & Spadea, S. (2020). MILDGLASS: GFRP Strands for Resilient Mild Prestressed Concrete (Project #207). In *NCHRP-IDEA Report to AASHTO Research and Innovation Committee*.

Rossini, M. (2019). *FRP Reinforcement for Prestressed Concrete Applications.* University of Miami. Link

Rossini, M., & Nanni, A. (2019). *MILDGLASS Demo Pile Project at 23rd Avenue Bridge over Ibis Waterway: Partially Prestressed Concrete Piles with GFRP Bars*. Miami. Link

Rossini, M., & Nanni, A. (2020). NCHRP IDEA/207 MILDGLASS: GFRP Strands for Resilient Mild Prestressed Concrete (Poster). In *Annual Meeting - Transportation Research Board (TRB-2020)*. Washington, DC. Link

Rossini, M., Pulvirenti, G., Spadea, S., & Nanni, A. (2018). *Final Report: Addition of FRP Design to LRFD Prestressed Beam Program Developed by FDOT*. Coral Gables, FL. Link